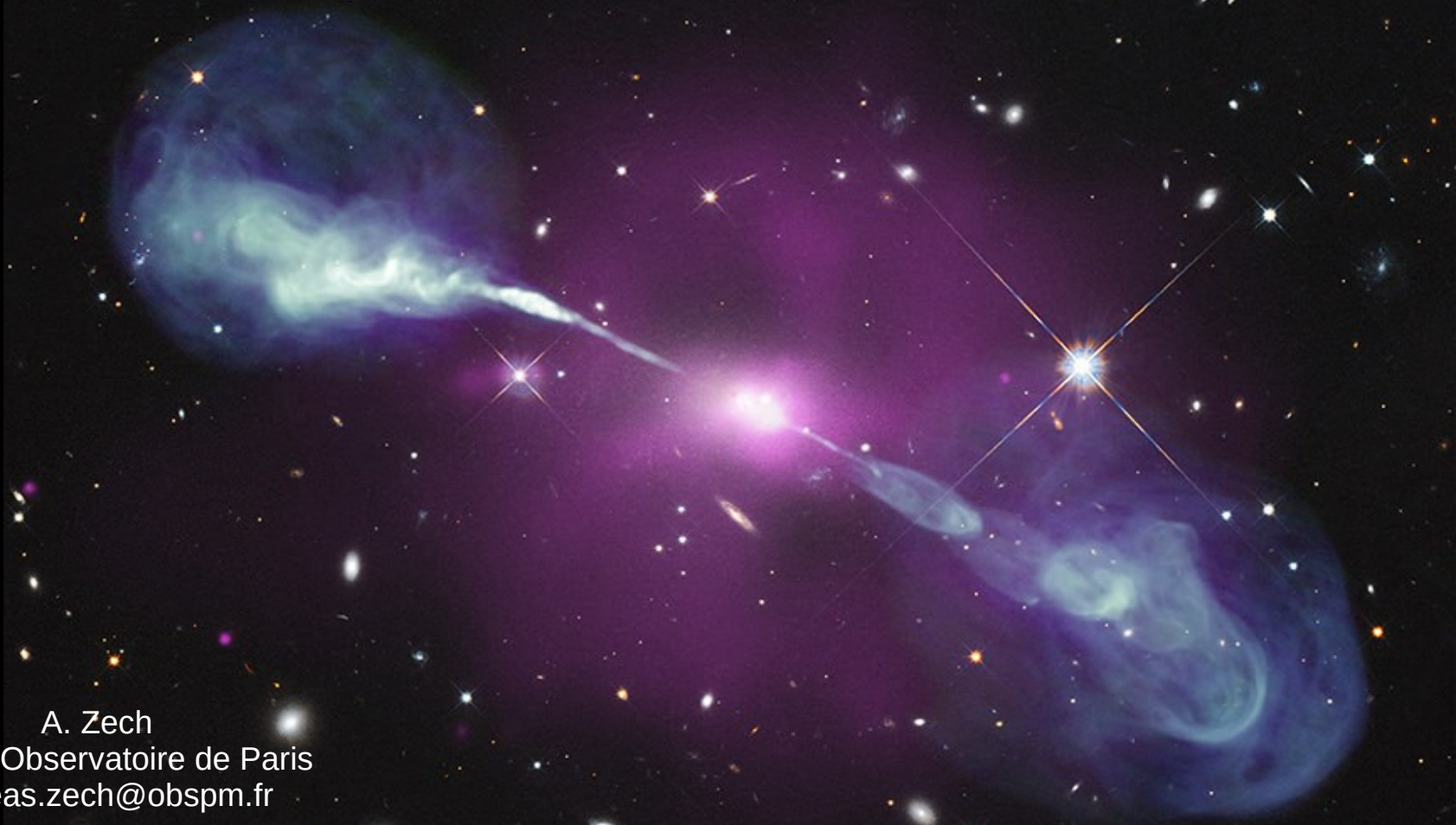


# Non-thermal emission from Active Galactic Nuclei



*Hercules A  
(NASA)*

A. Zech

LUTH – Observatoire de Paris  
andreas.zech@obspm.fr

“ École de GIF ”, APC, Paris  
Septembre 2024

# Content

---

## I non-thermal radiative processes

### 1) a short introduction to radiation

- basic quantities
- non-thermal processes

### 2) synchrotron radiation

- synchrotron emission and cooling
- cyclotron radiation, curvature radiation

### 3) Inverse Compton radiation

- IC emission and cooling
- Compton rocket and drag effects

### 4) pair production & annihilation

- basic characteristics
- pair cascades

### 5) pion-production and decay

- cross-section and emission spectrum

### 6) bremsstrahlung

## II variable emission from AGNs

### 1) a short introduction to AGNs

- structure of an AGN
- emission components
- AGN types

### 2) emission from blazars and radio-galaxies

- physics of relativistic jets
- emission mechanisms in the jet

### 3) rapid variability

- flux and polarisation variability in blazars
- variability in the one-zone model
- modelling of blazar flares


### 4) AGN flares and neutrinos

- what we have learnt from TXS 0506+056

### 5) conclusions & outlook

---

## II ) variable emission from Active Galactic Nuclei

A deep-field astronomical image of the Hercules A galaxy, showing two large, glowing pinkish-purple lobes connected by a central region. Two bright, narrow jets of light extend from the central region towards the lobes. The background is filled with numerous stars of various colors and sizes.

# 1) a short introduction to AGNs

# discovery of active galaxies

Active galaxies were first discovered in 1908 due to the very large width of their emission lines. “Seyfert galaxies” were seen to have line widths of up to  $\Delta v \sim 8500$  km/s , when interpreted as **Doppler broadening**.

(reminder :  $\frac{\Delta\lambda}{\lambda} \approx \frac{\Delta v}{c}$  )

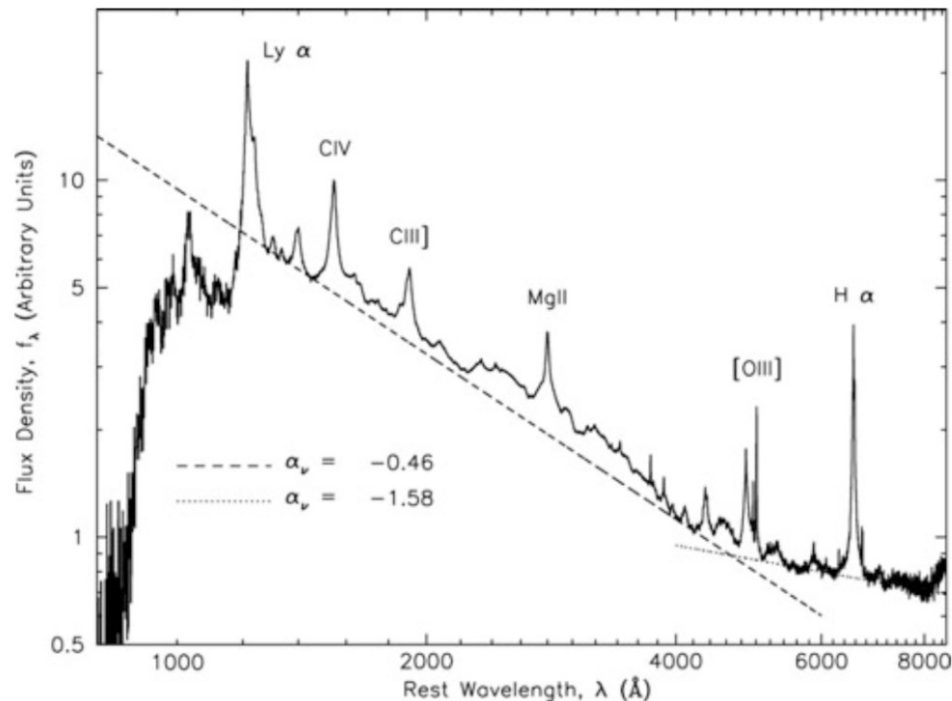
They show intense emission from unresolved core regions with radius  $r < 100$  pc.

For emission from a gravitationally bound gas

$$\Rightarrow v^2 \simeq \frac{GM}{r}$$

The broad emission lines from a very compact region imply thus a very large mass density in the core of such objects !

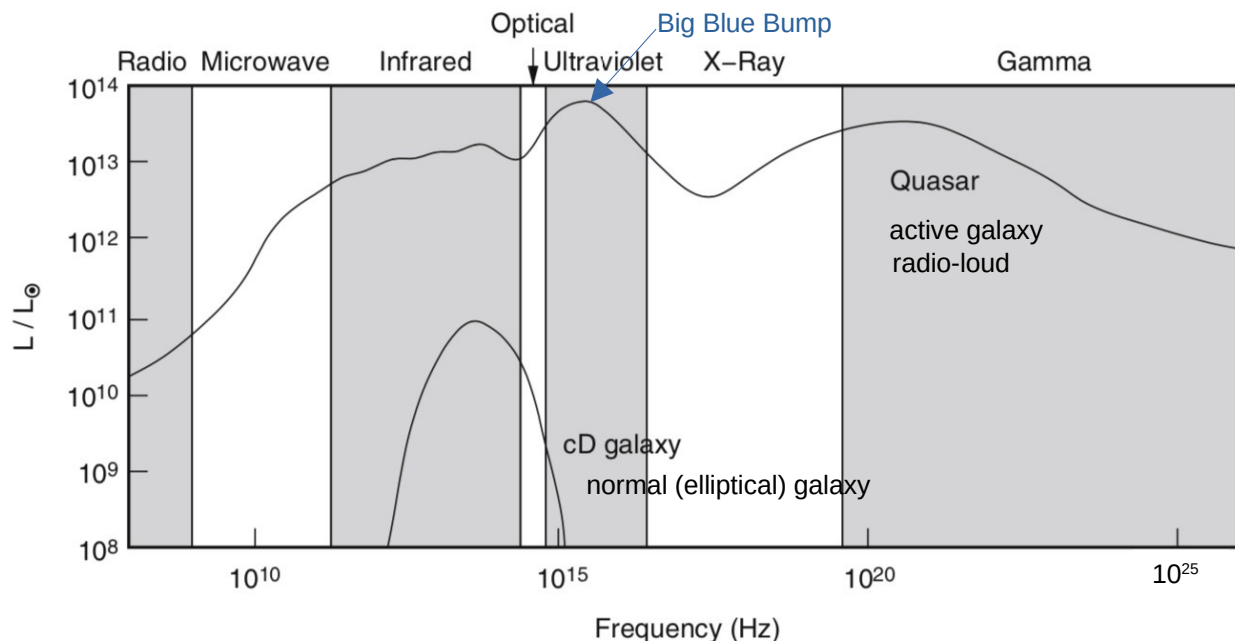
$$M(r) > 10^{10} \left( \frac{r}{100 \text{ pc}} \right) M_{\odot}$$



Combined optical spectrum of 2200 QSOs - a type of active galaxy - from the SDSS.

P. Schneider 2015

# discovery of active galaxies



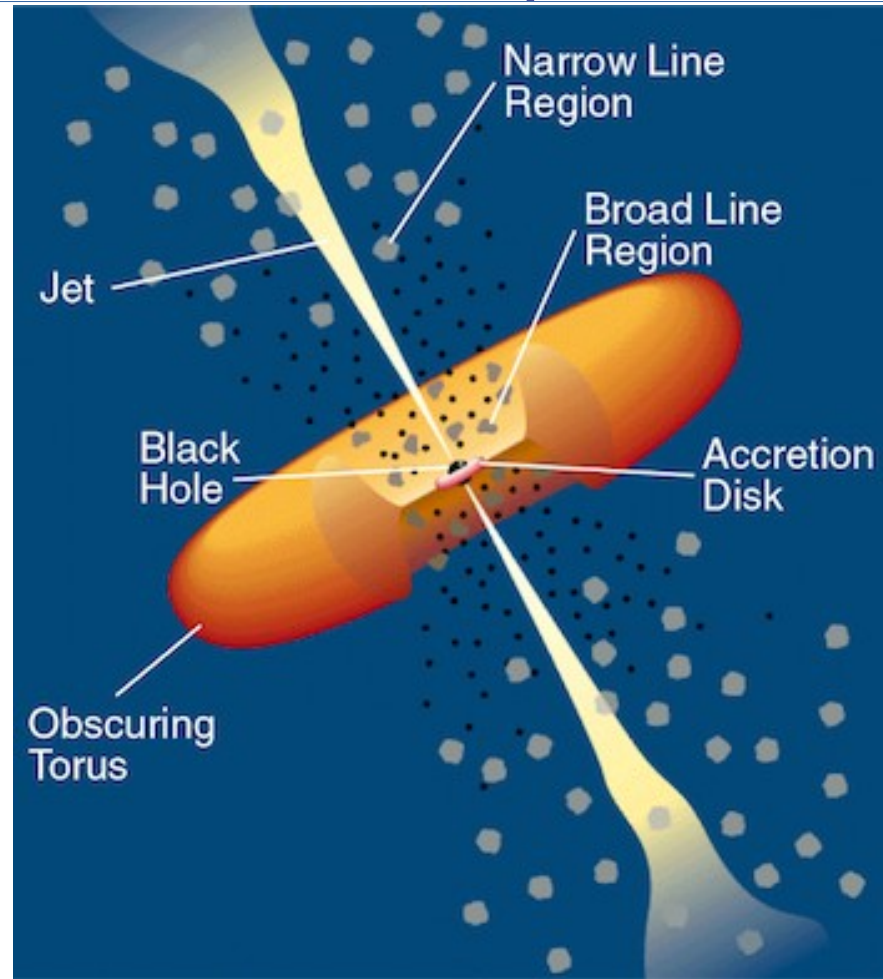
P. Schneider 2015

Active galaxies were found to have a vastly **larger spectrum** than normal galaxies. Some classes emit from the radio band up to very-high energies.

Their spectral continuum can be approximated with **power laws** in different spectral bands, which indicates a **non-thermal** origin for their emission. Their emission was also found to be polarised.

Active galaxies show in general **rapid flux variability** - more rapid with shorter wavelengths.

# AGN components



*Trevor C. Weekes, Very High Energy Gamma-Ray Astronomy*

# AGN components: central engine - SMBH

The compact, high-luminosity center of active galaxies has been identified with a *central engine* in the form of a **super-massive black hole (SMBH) accreting nearby matter**.

The existence of a black hole is necessary for energetic reasons:

- luminosity  $L \sim 10^{47} \text{ erg / s}$   
lifetime (from extension of radio lobes)  $\Delta t > 10^7 \text{ yr}$   
-> energy requirement  $E_{\text{req}} \sim 3 \times 10^{61} \text{ erg}$
- size of the central engine:  $R < 3 \times 10^{15} \text{ cm}$   
(from observations of flux variability on the time-scale of a day)

If one assumes this energy was gained by fusion:

- max. efficiency  $\epsilon \sim 0.8\%$  :  $\epsilon m c^2 \sim E_{\text{req}}$  ->  $m \sim 2 \times 10^9 M_{\odot}$ .
- Such a massive object has a Schwarzschild radius  $r_s \sim 6 \times 10^{14} \text{ cm}$

A SMBH seems the only possible candidate and in this case, gravitational energy production is far more efficient than nuclear fusion:  
 $\epsilon \sim 6\%$  for Schwarzschild BH,  $\epsilon$  up to 29% for Kerr BH.



*first direct image of the central black hole of M87 with EHT  
(EHT Collaboration)*



# AGN components: central engine - accretion disk

## accretion:

Gas falling onto a compact object sees its potential (gravitational) energy converted into kinetic energy.

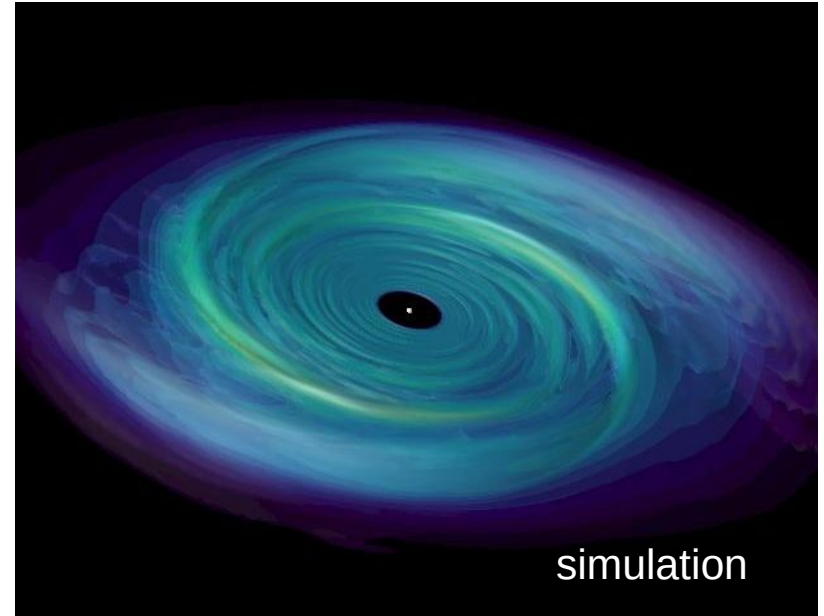
In general, the gas has finite angular momentum and, through internal friction, settles into an accretion disk oriented perpendicularly to the angular momentum vector.

The disk rotates differentially following Kepler's laws. This causes friction that heats the disk and leads to a deceleration. The gas moves slowly inwards and more potential energy is converted first into kinetic energy and then internal energy (heat) that is radiated away.

## geometrically thin, optically thick disk:

One can show that, in a first approximation, a geometrically thin, optically thick disk radiates as a superposition of Planck spectra with a radial temperature profile following :

$$T(r) = \left( \frac{3c^6}{64 \pi \sigma_{SB} G^2} \right)^{1/4} \dot{m}^{1/4} M_{BH}^{-1/2} \left( \frac{r}{r_s} \right)^{-3/4}$$



<https://apod.nasa.gov/apod/ap050312.html>

with  $\dot{m}$  the mass accretion rate and

$$r_s = \frac{2GM_{BH}}{c^2} \text{ the Schwarzschild radius.}$$

In AGNs, accretion disks radiate mostly in the UV range (leading to a “big blue bump” in the spectrum).

# Eddington accretion rate

For matter to be able to fall into the gravitational potential, the radiation force from the emitted light must be smaller than then gravitational force. One considers a fully ionised gas falling onto an isotropic radiation field. The principal interaction is through **Thomson scattering of electrons**:

$$F_{rad} = \sigma_T \frac{L}{4 \pi r^2 c}$$

The gravitational force on the plasma is dominated by the protons :

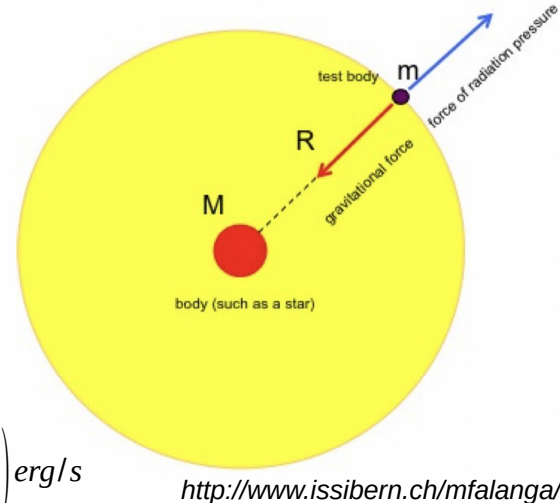
$$F_{grav} = \frac{G M_{BH} m_p}{r^2}$$

Accretion proceeds as long as  $F_{rad} < F_{grav}$  i.e.  $L < \frac{4 \pi G c m_p}{\sigma_T} M_{BH} \equiv L_{edd} \approx 1.26 \times 10^{38} \left( \frac{M_{BH}}{M_{\odot}} \right) \text{erg/s}$

This defines the **Eddington luminosity** of a black hole with given mass. Inversely, this relation provides a lower limit for the mass of SMBH for a given luminosity. Luminous AGN have typically  $M_{BH} > 10^8 M_{\odot}$  , while less luminous ones have  $M_{BH} > 10^6 M_{\odot}$  .

If the efficiency  $\epsilon$  of conversion from potential energy to radiation is known, the mass accretion rate is given by

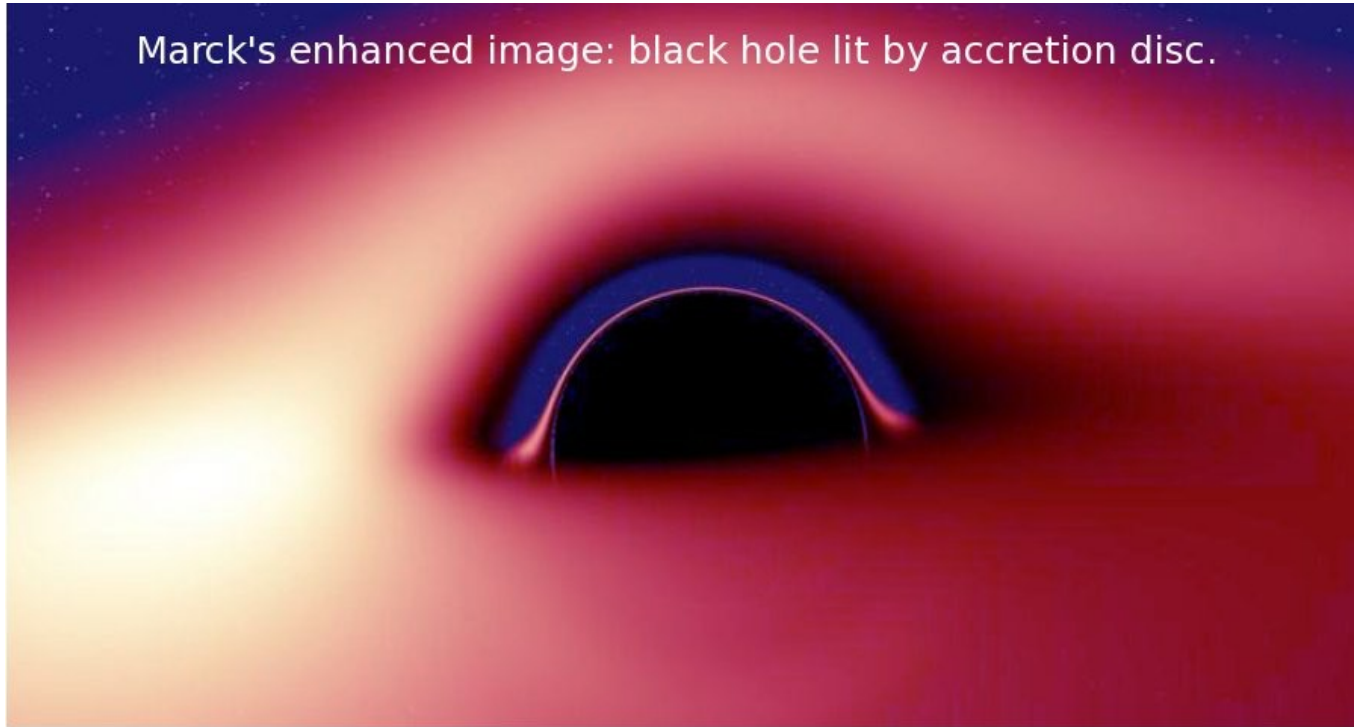
$$\dot{m} = \frac{L}{\epsilon c^2} \approx 0.18 \frac{1}{\epsilon} \left( \frac{L}{10^{46} \text{erg/s}} \right) M_{\odot} / \text{yr} \quad \text{and its maximum is} \quad \dot{m}_{Edd} = \frac{L_{Edd}}{\epsilon c^2} \approx \frac{1}{\epsilon} 2 \times 10^{-9} M_{BH} / \text{yr}$$



# AGN components: central engine - accretion disk

Marck's enhanced image: black hole lit by accretion disc.

approaching side  
(blueshift)



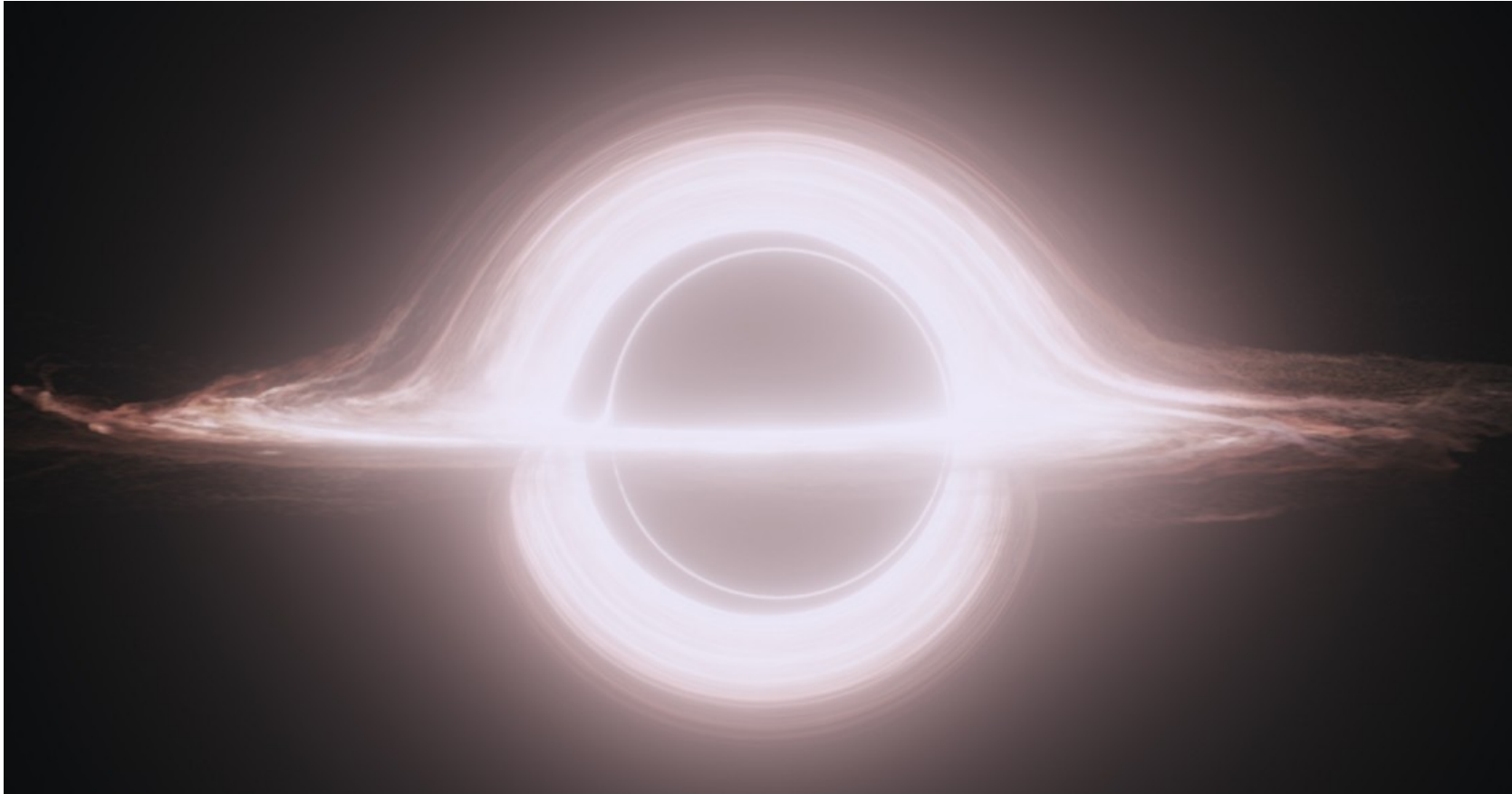
receding side  
(redshift)

simulated view of an accretion disc  
incorporating all relativistic effects  
*wikipedia, image J.A. Marck, OP, 1995*

# AGN components: central engine - accretion disk

---

the  
Hollywood  
version



Gargantua: A variant of the black-hole accretion disk seen in the film Interstellar. Credit: DNEG/Warner Bros. Entertainment Inc./CQG 32 065001

# AGN components: corona

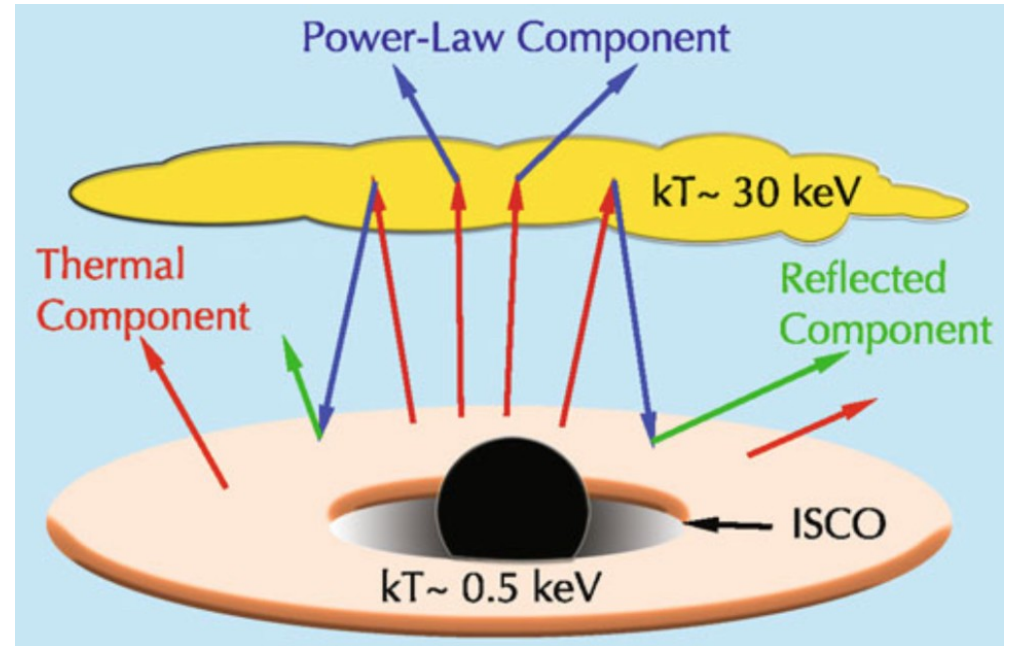
An additional emission of **X-rays** comes from the close vicinity of the disk.

In analogy to stellar atmospheres, a hot layer of gas is expected to form above the optically thick disk - the **corona**. This gas is optically thin and does not cool efficiently. It is expected to have a very high energy (10s to 100s of keV), maybe reaching the *virial temperature*:

$$k_B T \approx G M_{BH} m / r$$

Photons from the disk can be up-scattered in this gas via the *Inverse Compton effect*. The corona emits these up-scattered photons in the form of a power law with a cut-off at  $\sim 100$  keV.

In addition, part of the photons from the corona are emitted back towards the disk and form a “**reflected component**”. These photons are down-scattered in energy on the electrons in the disk.



P. Schneider 2015

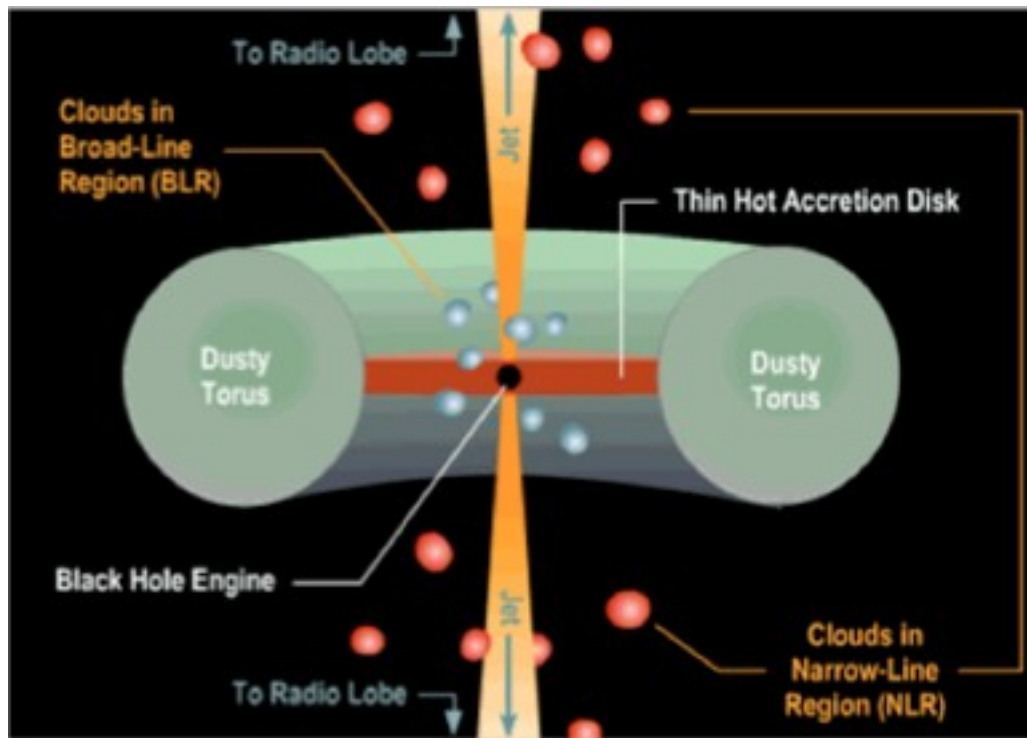
# AGN components: broad line region

The broad emission lines detected from many active galaxies must come from a gas of very high velocity ( $\sim 10\,000$  km/s). This gas seems to be located close to the central engine, since for Keplerian motion in the gravitational potential:

$$v_{rot} = \sqrt{\frac{GM_{BH}}{r}}, \text{ thus } r \sim 500 r_s \text{ (sub-pc range).}$$

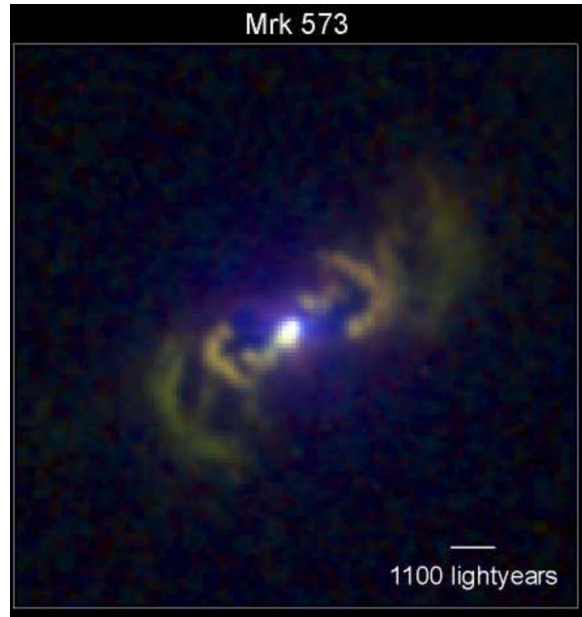
The **broad line region (BLR)** seems to consist of a very large number of fast-moving dense clouds of a typical temperature  $T \sim 20\,000$  K. They are partially ionised through radiation from the central engine.

Characteristics of this medium are deduced from observations of the emission lines (width, intensity, absence of forbidden lines,...).

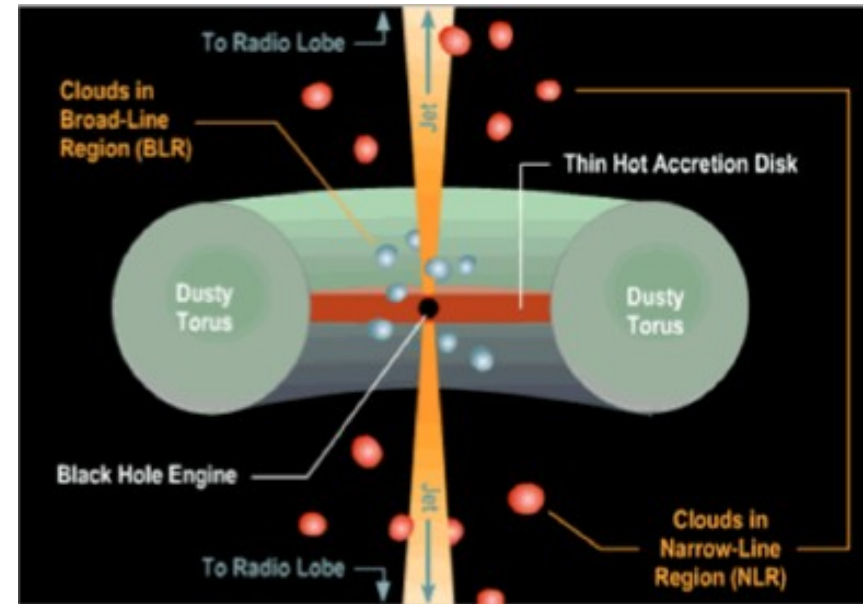


<http://ay20-eric.blogspot.com/2011/10/clarifications-on-agn.html>

# AGN components: narrow line region



HST, NASA, <http://www.astro.ru.nl/~falcke/trans1.jpg>



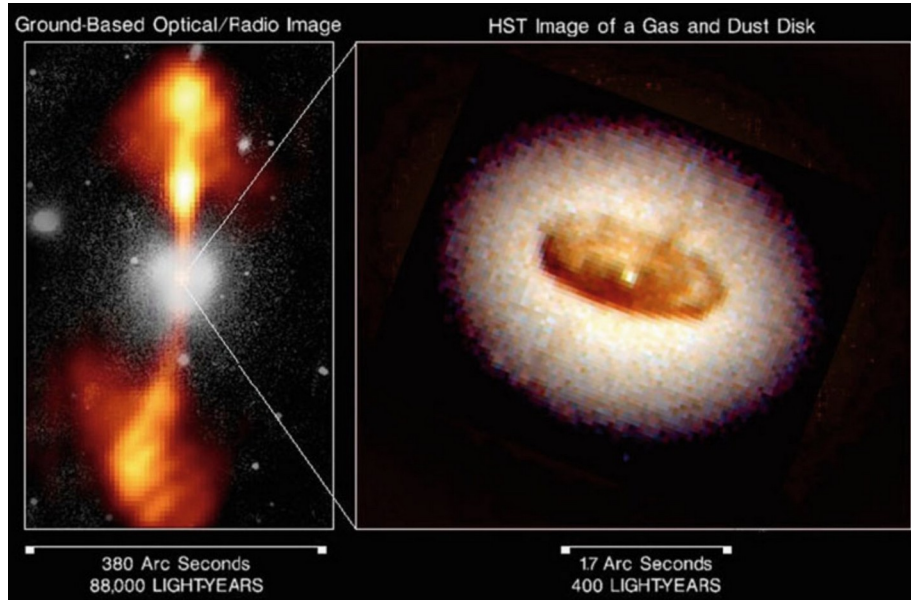
<http://ay20-eric.blogspot.com/2011/10/clarifications-on-agn.html>

Most AGNs emit also narrow lines, with typical widths  $\sim 400$  km/s. These include the “forbidden” [OIII] line, indicating that the **narrow line region (NLR)** is much less dense than the BLR.

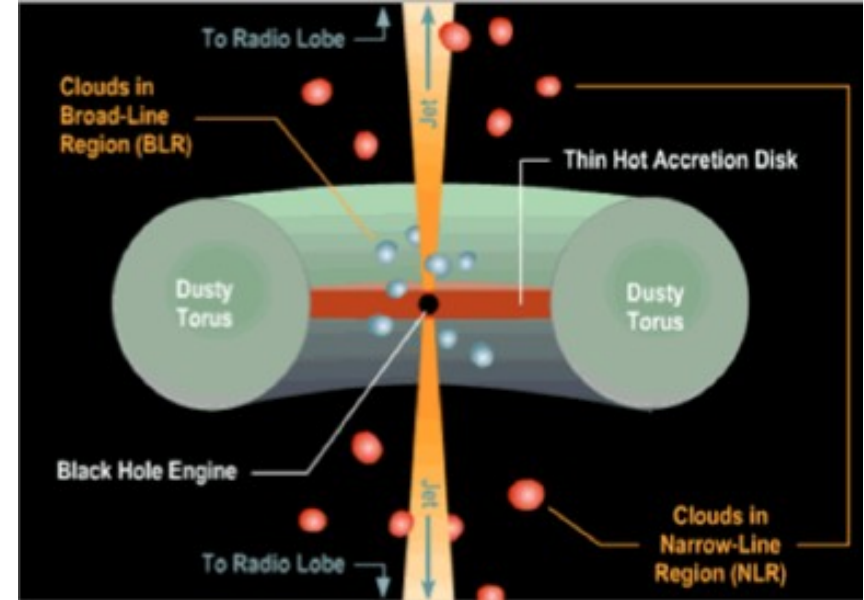
The NLR is thought to extend to  $\sim 100$  pc and to consist of clouds as well. The gas temperature is  $T \sim 15\,000$  K. It can be spatially resolved in certain Seyfert galaxies and shows the shape of two cones above and below the disk.

It seems that the ionisation of the gas in the NLR is not isotropic, but occurs in “ionisation cones”.

# AGN components: dusty torus



P. Schneider 2015



<http://ay20-eric.blogspot.com/2011/10/clarifications-on-agn.html>

In the current picture, a torus of gas and dust surrounds the accretion disk, with a size about an order of magnitude larger than the BLR. It consists of dense clouds. The dust in these clouds absorbs radiation from the central engine in the direction of the plane of the accretion disk. This leads to heating of the torus, which radiates in the **infrared**.

The **dusty torus** is difficult to observe directly and its characteristics are not well known. Its temperature would be  $T \lesssim 1000$  K, limited by the dust sublimation temperature.

It plays an important role in the AGN unification scheme since it obscures emission for certain viewing angles.



# AGN components: relativistic jet

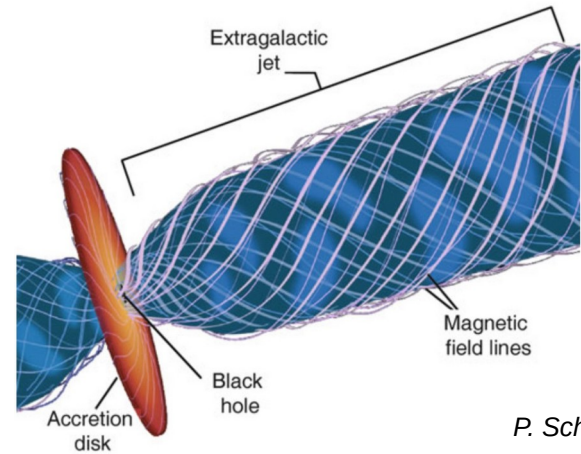
A small fraction of AGNs (~10%) are qualified as “**radio-loud**” and present a significant **non-thermal emission** from relativistic jets.

They consist of relativistic plasma (pair plasma or ion-electron plasma) carrying magnetic fields. A **magnetic field with a helical large-scale structure** is thought to assure their stability.

AGN jets are found at scales of **pc to kpc**. They can even extend to **Mpc scales** where they end in large radio lobes.

Jets emit electromagnetic radiation over a very large frequency range. From radio to UV/X-rays it is due to **synchrotron radiation**.

At larger frequencies (X-rays up to very high energies), it is probably due to **Inverse Compton emission** (or hadronic emission processes).



*P. Schneider 2015*

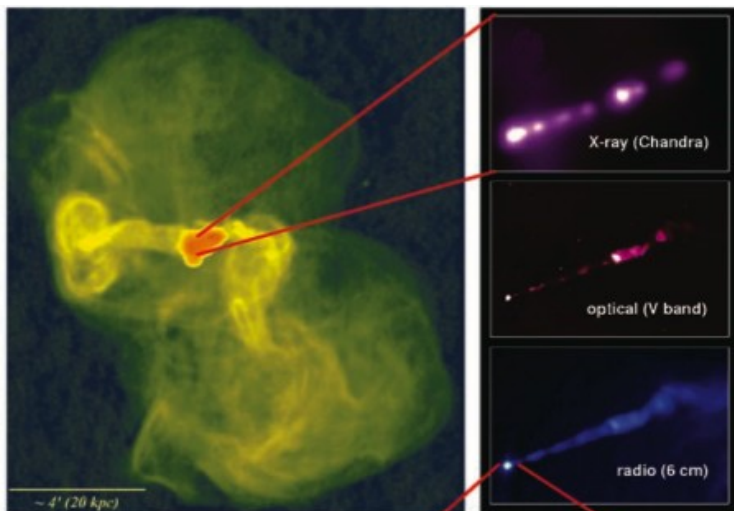


M87, HST

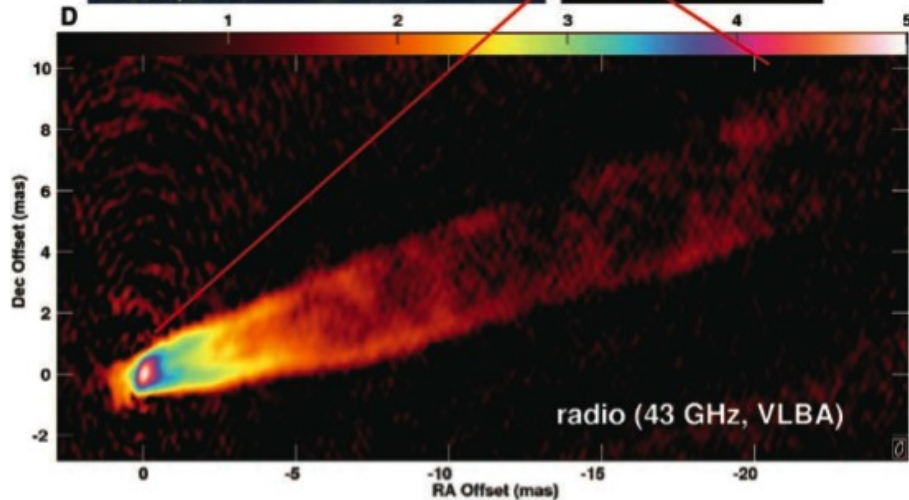


# M87 - a close look at a radio galaxy

VLA radio emission shows **kpc jets and radio lobes**



synchrotron emission from the **plasma jet, its core and bright knots** seen by Chandra, HST, VLA (size  $\sim 2$  kpc)

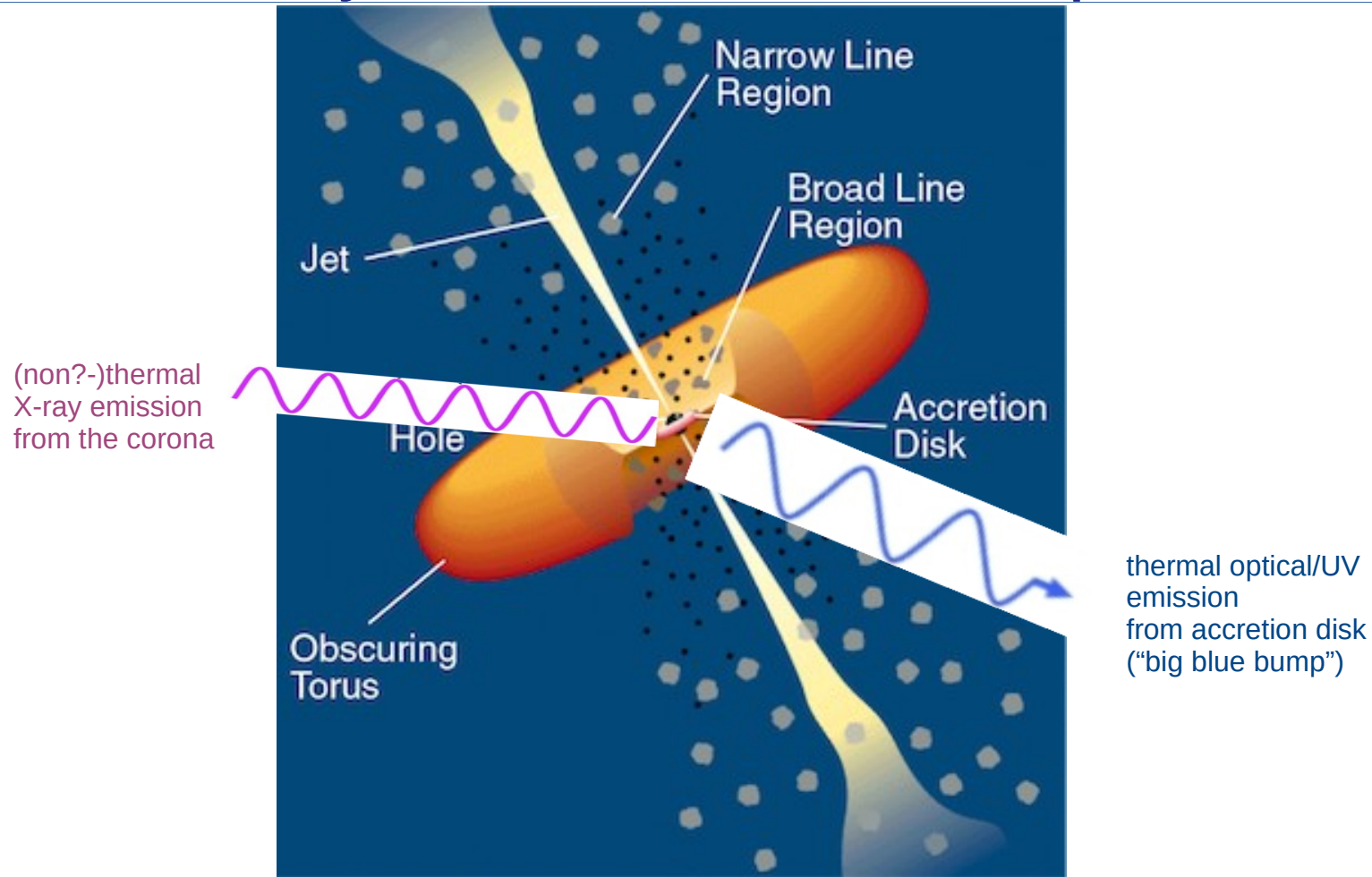


**inner jet and core** resolved by VLBA

The central black hole is thought to be found at a few  $10 R_s$  from the radio core at 43 GHz.

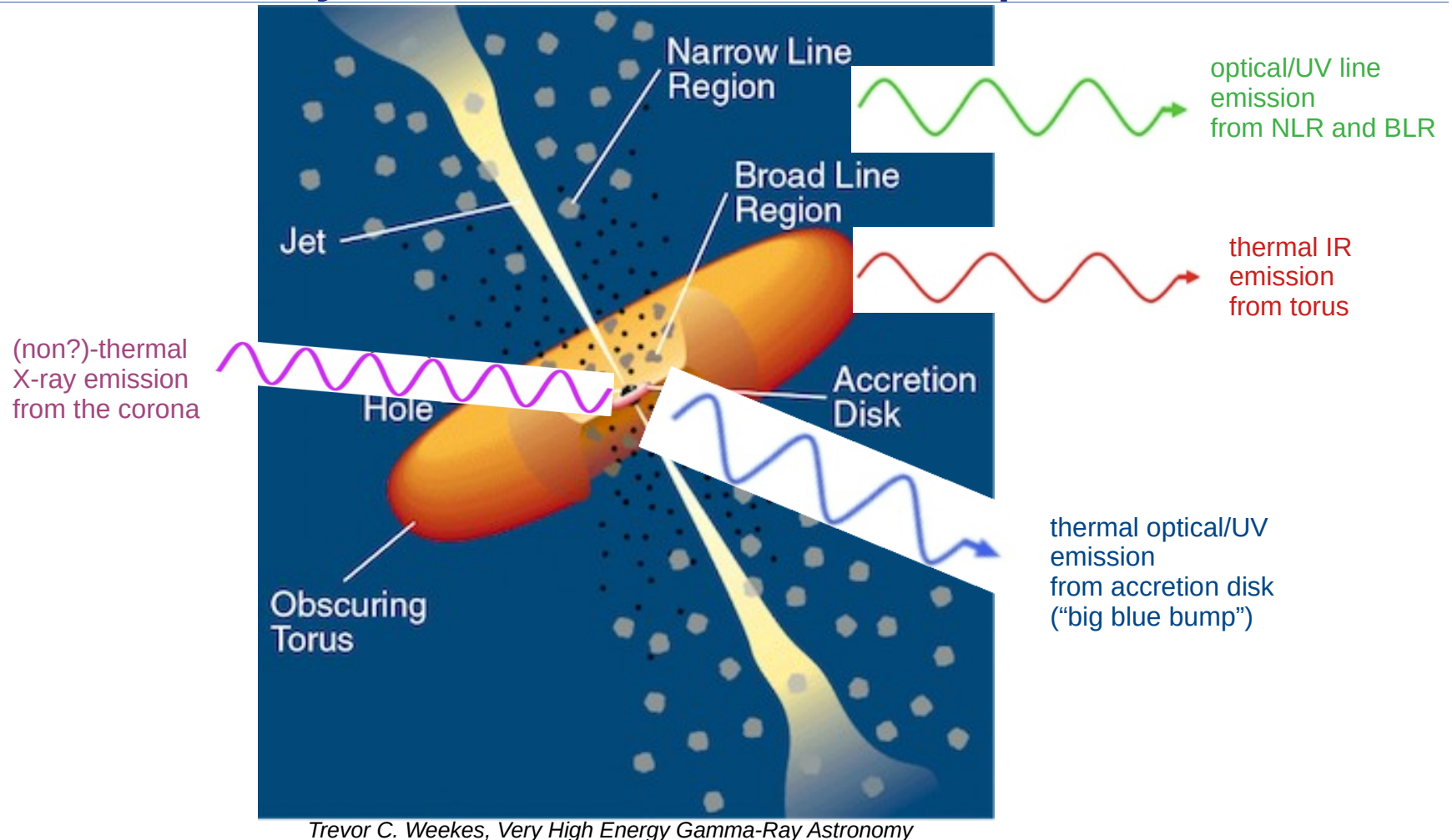
Veritas, HESS...,  
*Science*, 325, 444  
(2009)

# summary: AGN emission components

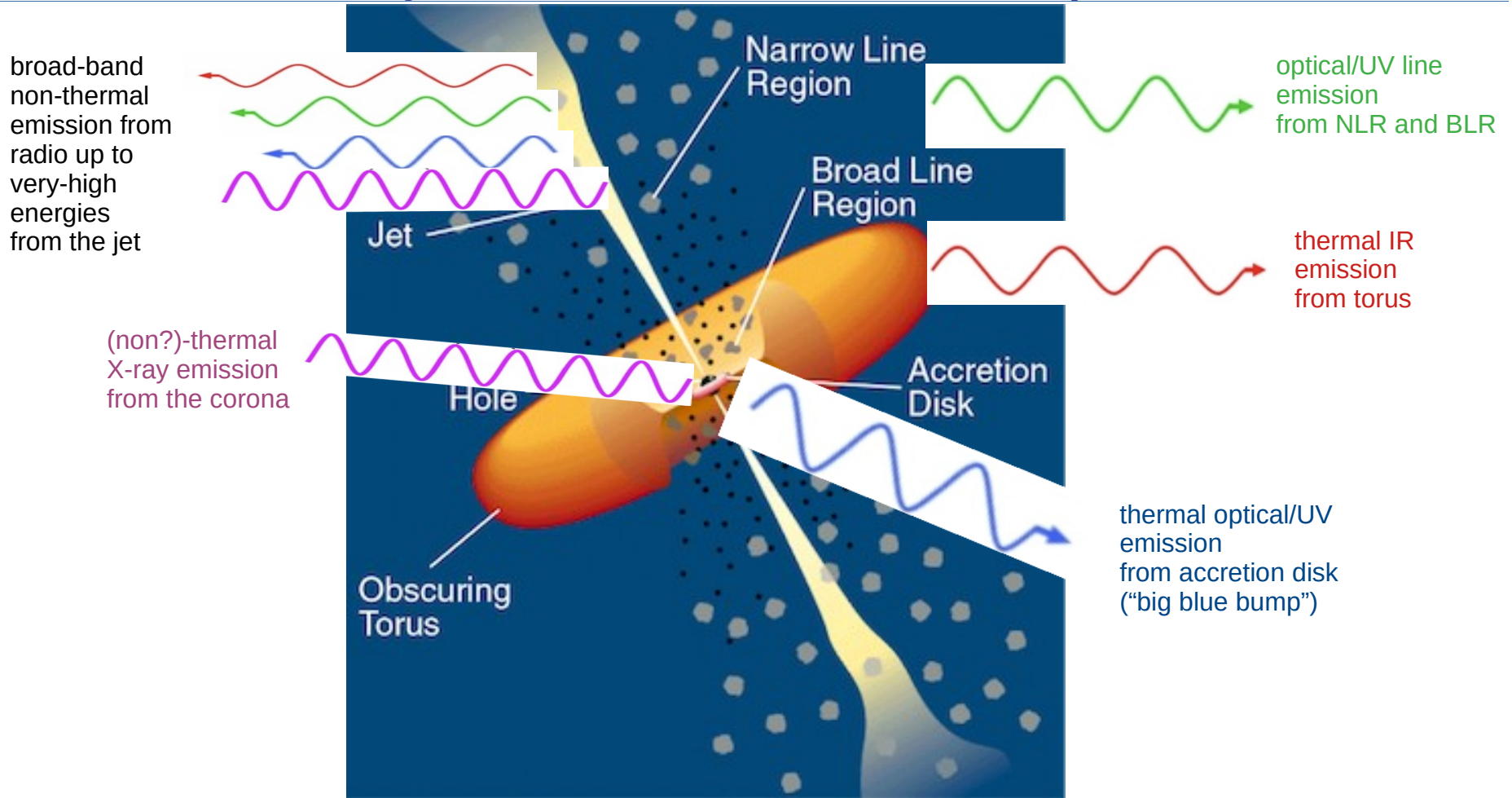


*Trevor C. Weekes, Very High Energy Gamma-Ray Astronomy*

# summary: AGN emission components



# summary: AGN emission components



Trevor C. Weekes, *Very High Energy Gamma-Ray Astronomy*

# AGN unified model

The unified model attempts to explain the large number of different AGN classes with a single physical object.

**Dichotomy** of “radio-loud” (jetted) and “radio-quiet” AGN.

Other differences in the observed emission (mostly) due to **viewing angle**:

- **large angle (close to disk plane):**

View of the BLR is obstructed by the dusty torus. Spectra show only narrow emission lines. (*Narrow-Line Radio Galaxies, Seyfert 2*)

- **intermediate angle:**

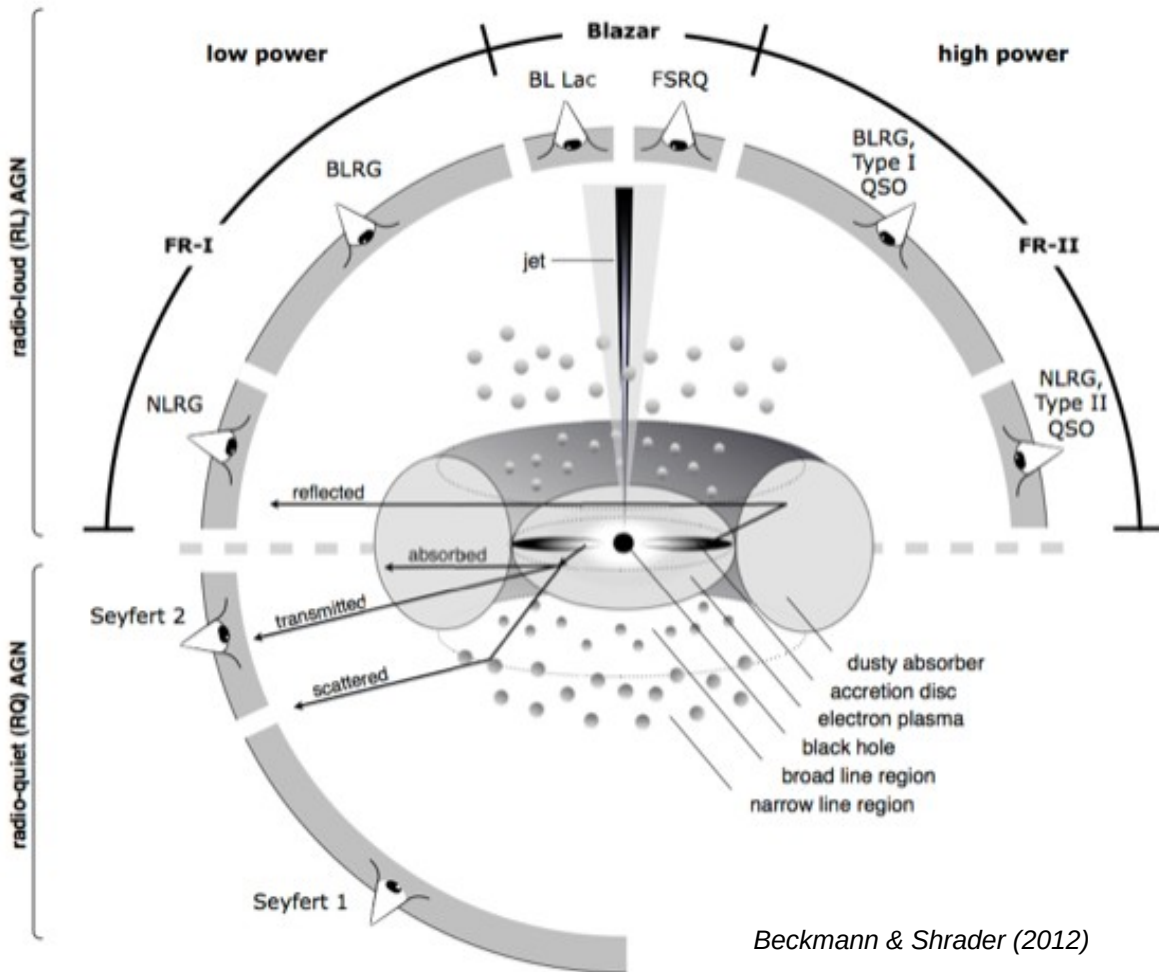
Broad emission lines can be observed. (*Broad-Line Radio Galaxies, Seyfert 1*)

- **small angle (closer to jet axis or disk normal):**

Bright emission from the central region (*radio-quiet & radio-loud quasars or QSOs*)

- **very small angle (~aligned with jet axis):**

For radio-loud objects, relativistic effects amplify the observed luminosity and reduce variability time scales. (*blazars*)



# a few specimen

Galaxy NGC 7742

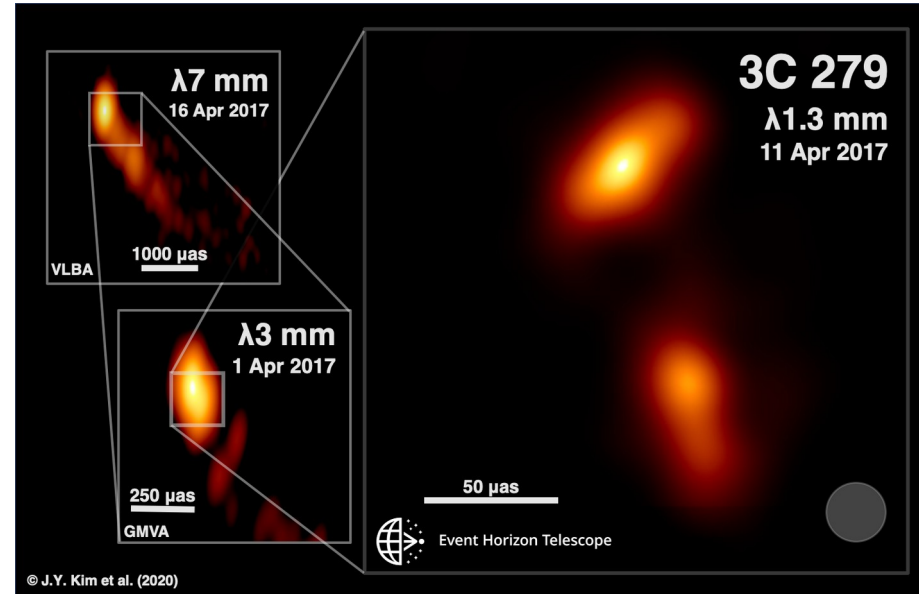


Hubble  
Heritage

PRC98-28 • Space Telescope Science Institute • Hubble Heritage Team

*the Seyfert galaxy NGC 7742 Image credit: Hubble Heritage Team (AURA/STScI/NASA)*

the blazar Mrk 421  
(Sloan Digital Sky Survey)

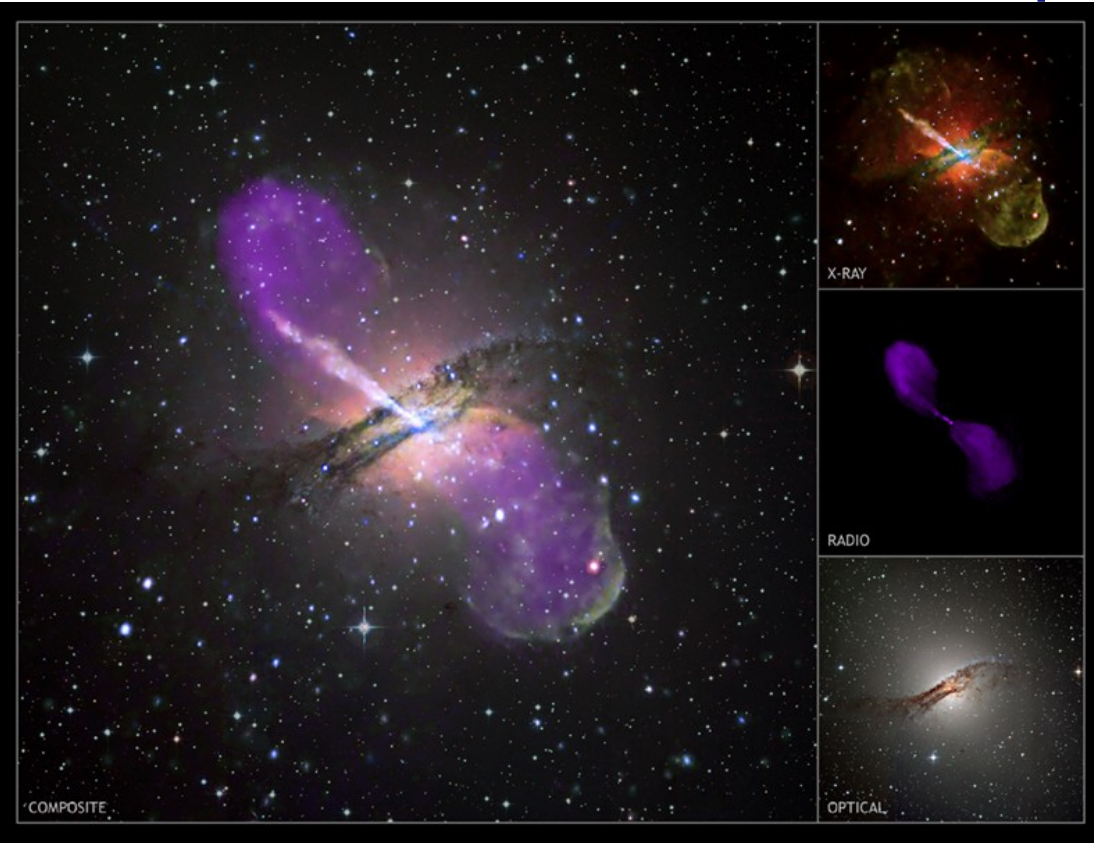


the blazar 3C 279

Credit: J.Y. Kim (MPIfR), Boston University Blazar Program (VLBA and GMVA), and the Event Horizon Telescope Collaboration



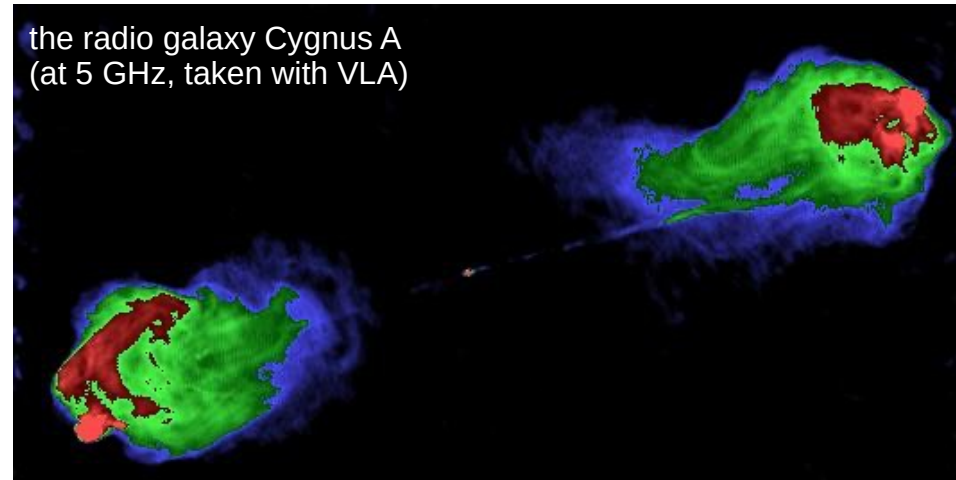
# a few specimen



the radio galaxy M87  
(NASA and The Hubble  
Heritage Team  
(STScI/AURA) )

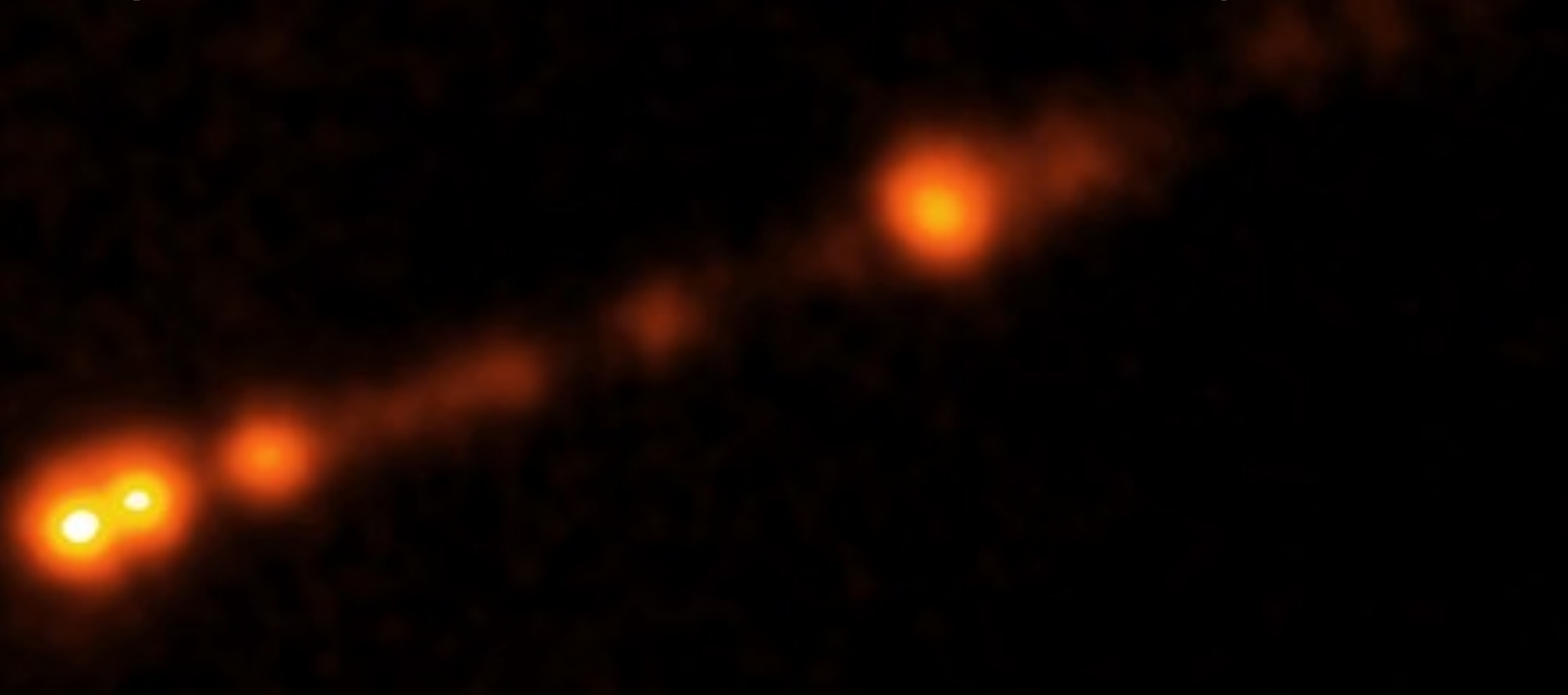


the radio galaxy Cygnus A  
(at 5 GHz, taken with VLA)



the radio galaxy Centaurus A  
(Credit: X-ray: NASA/CXC/CfA/R.Kraft et al; Radio:  
NSF/VLA/Univ.Hertfordshire/M.Hardcastle; Optical:  
ESO/WFI/M.Rejkuba et al.)

## 2) emission from blazars and radio-galaxies



# broad-band jet emission : steady-jet model

The steady-jet model by *Blandford & Königl (1979)* explains the observed flat emission spectrum ( in spectral flux density  $F_\nu$  [ $\text{erg s}^{-1} \text{cm}^{-2} \text{Hz}^{-1}$ ] ) through the **sum of synchrotron emission spectra** from a non-thermal electron plasma follow adiabatic expansion, leading to a conical jet.

Magnetic field strength and electron density decrease along the jet.

The lower region of the jet is **optically thick** to radiation of all frequencies. In the middle region, the jet becomes optically thin to radiation of progressively lower frequencies.

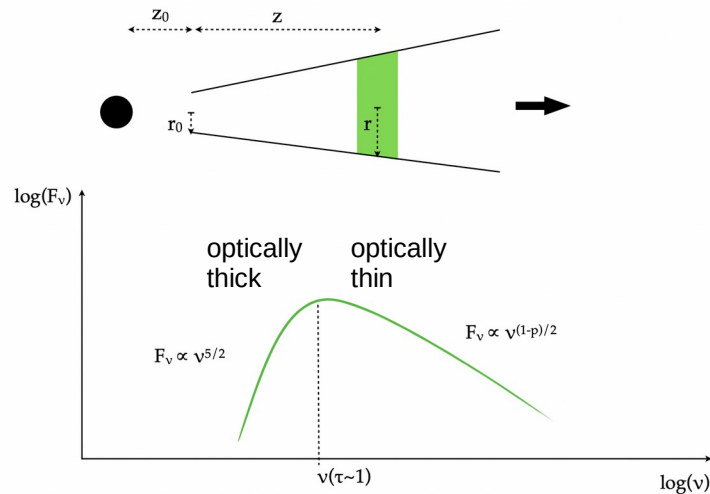


FIGURE 1.9 – Densité spectrale d'énergie d'une couche de jet de rayon  $r$  située à une distance  $z$  de la base.

M. Péault, PhD thesis 2019

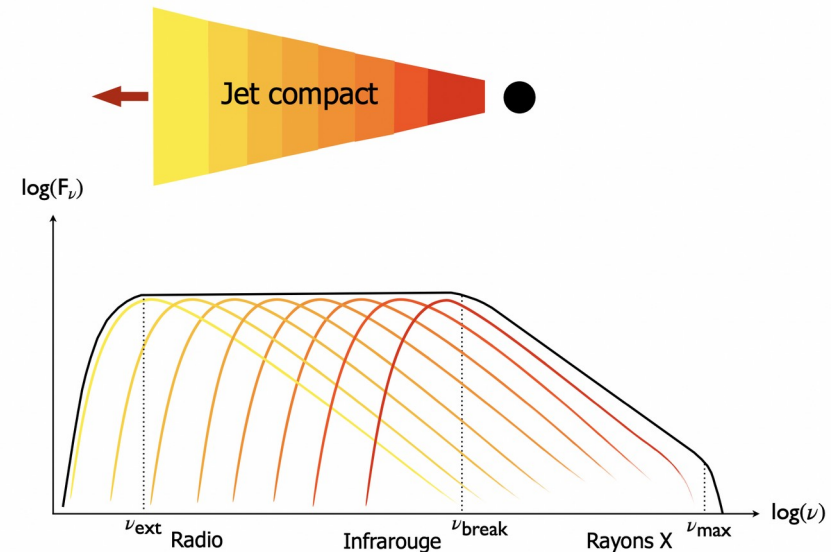
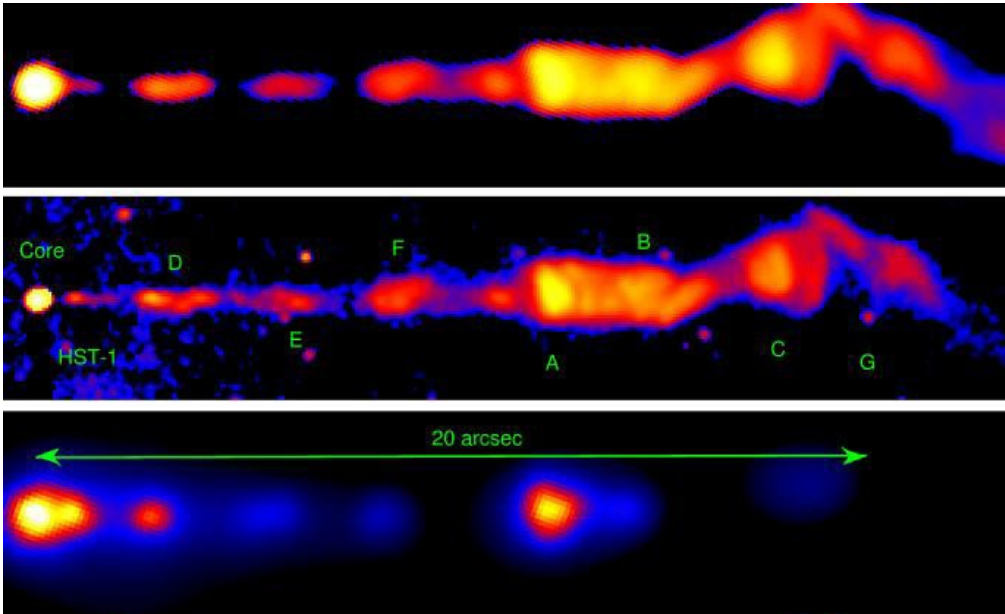
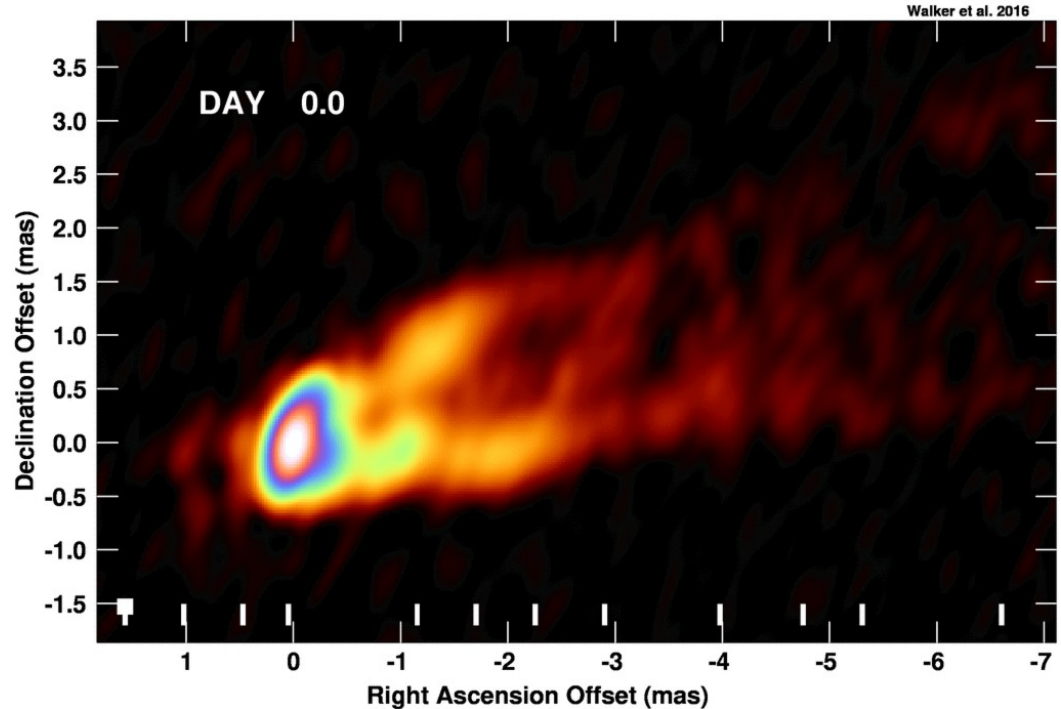


FIGURE 1.10 – Spectre d'émission du jet d'après le modèle de Blandford et Königl.

# broad-band jet emission : observations



Multi-wavelength view of the M87 jet. From top to bottom:  
radio (VLA), optical (HST), and X-ray (Chandra)  
(Marshall et al. 2002)



VLBI images of the M87 radio core  
(Walker et al. 2016)

Jets from AGN are not homogeneous :

- standing and moving “knots” are seen from radio to X-ray bands
- some “knots” have superluminal velocities

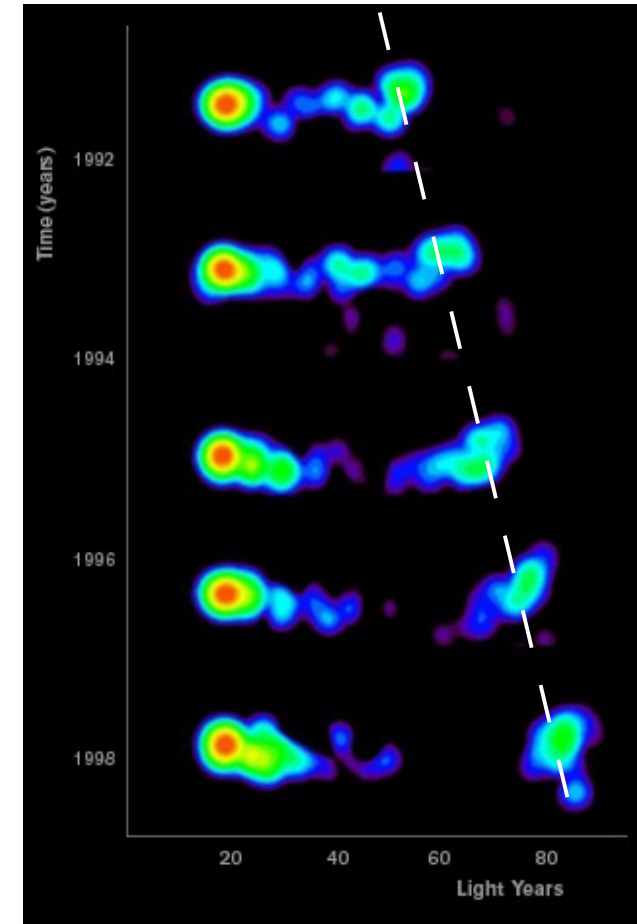
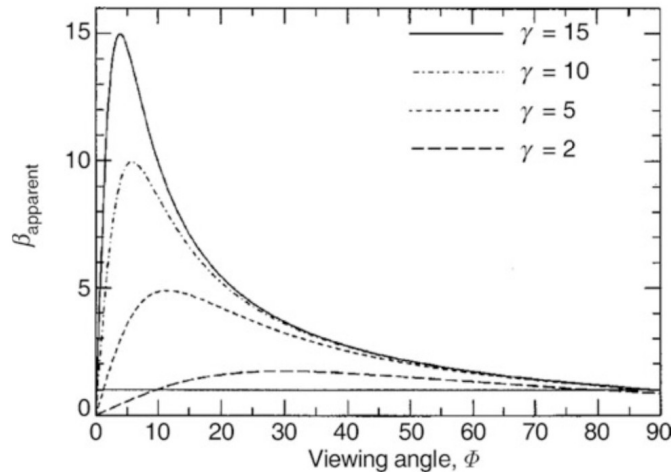
# superluminal motion

Apparent superluminal motion of components observed in some AGN with very long baseline interferometry (VLBI) helped identify the existence of relativistic jets.

The apparent movement of components with  $v_{app} > c$  (sometimes  $v_{app} = 6c$  or more !), is caused by the projection of emission from a relativistic jet pointing in our direction on the celestial plane.

$$v_{app} = \frac{v \sin \phi}{1 - \beta \cos \phi}$$

with  $v = \beta c$  the real velocity of the component along the jet and  $\phi$  the viewing angle of the jet



<http://user.astro.columbia.edu/~jules/UN2002/superluminal.html>

# superluminal motion explained

Demonstration:

- A “radio knot” is emitted from position A of the jet at  $t = 0$ . Its distance from A at time  $t = t_e$  is  $v t_e$  (position B).

We only observe the movement projected onto the sky, i.e. its transverse component  $\Delta r = v t_e \sin \phi$  (from C to B).

- Photons emitted from the new position B will take slightly less time to reach the observer. For the observer, the time interval between the signal from A and from the new position B is :

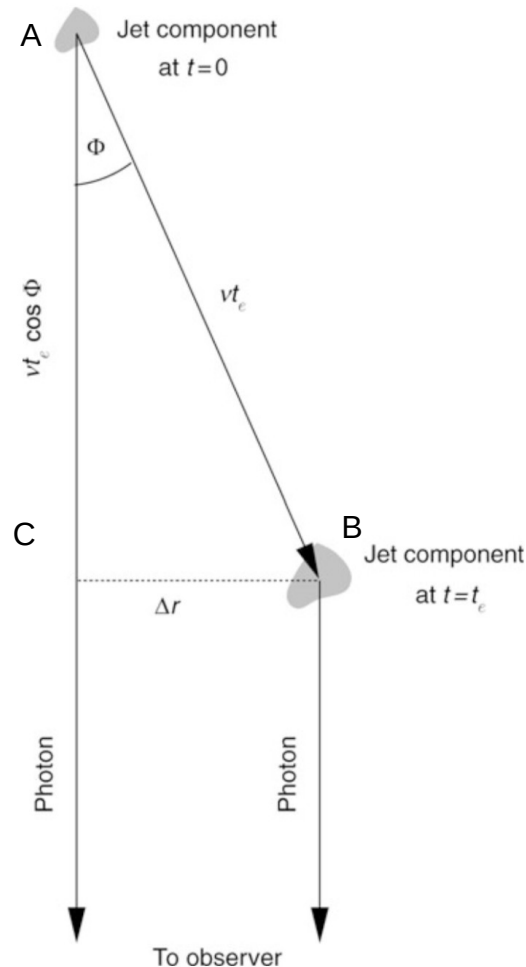
$$\Delta t = t_e - \frac{v t_e \cos \phi}{c} = t_e (1 - \beta \cos \phi)$$

- with  $v_{app} = \frac{\Delta r}{\Delta t}$  one obtains the above equation for  $v_{app}$ .

- For a given  $v$ , the maximum value of  $v_{app}$  is achieved if

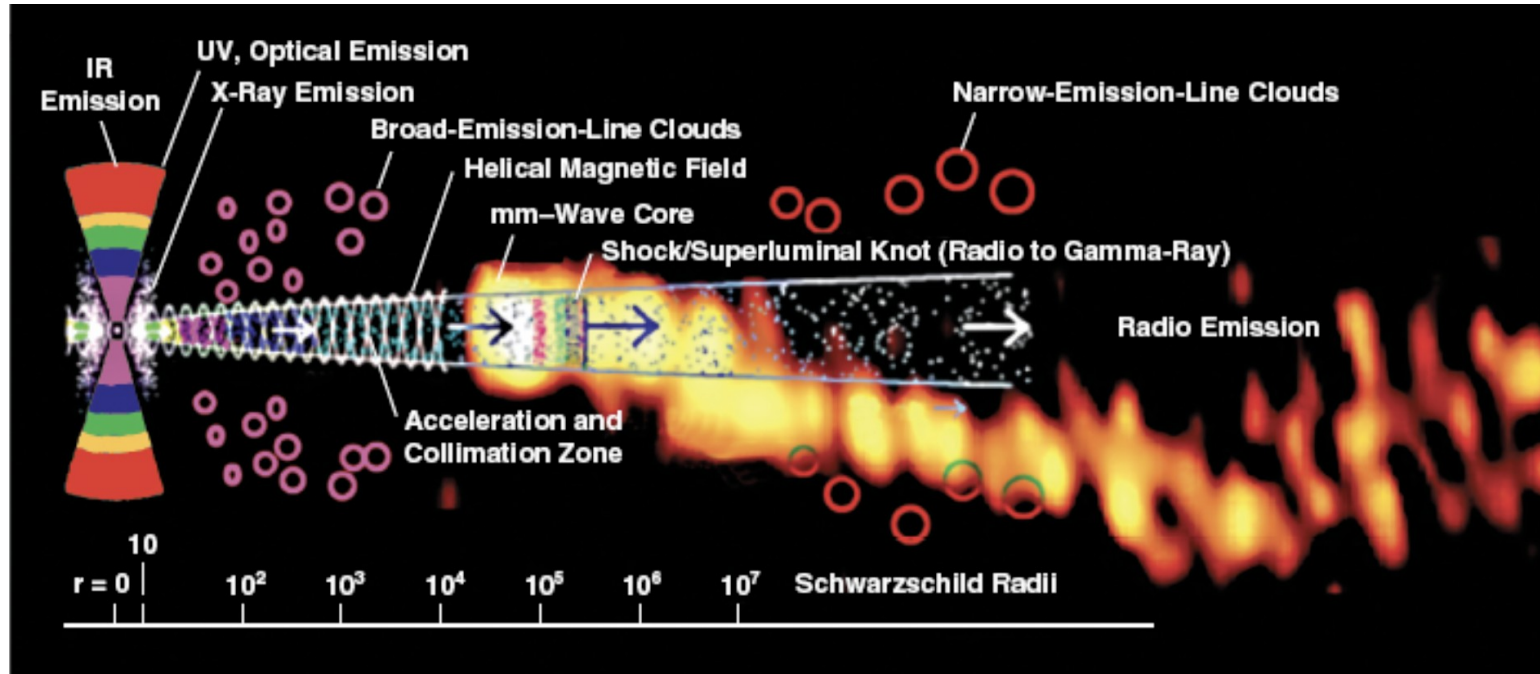
$$\sin \phi = 1/\gamma \quad \text{with the Lorentz factor} \quad \gamma = \frac{1}{\sqrt{1-v^2/c^2}}$$

This leads to  $v_{app,max} = \gamma v$ .



# broad-band jet emission : the current picture

Overlay of a 3 mm radio image of the blazar 3C454.3 (Krichbaum, et al. 1999) on a diagram of a quasar from Marscher et al. (2008), not to scale.  
A. E. Wehrle 2009



current standard picture of the inner jet (A. Marscher 2008), derived from VLBI and polarisation measurements :

- acceleration/collimation region with helical magnetic field and spiral streamlines  
→ emission region of high-energy emission ?
- conical standing shock (= recollimation shock?) is identified as the mm-wave core (VLBI core), from which superluminal knots are seen to detach.
- the position of the radio core does not coincide with the base of the jet, but is shifted due to frequency-dependent self-absorption (“core shift”)

# relativistic beaming

---

Emission from relativistic jets is subject to several relativistic effects :

- **Doppler effect:** Light emitted from a jet pointing at the observer under an angle  $\Phi$  is blue-shifted

$$\nu_{obs} = \delta \nu_{em} \quad \text{by the Doppler factor} \quad \delta = \frac{1}{\gamma(1 - \beta \cos \phi)}$$

- **relativistic beaming** : Light emitted isotropically in the reference frame of the moving knot is emitted preferentially in the direction of movement of the plasma in the observer frame. This leads to an amplification (“Doppler boosting”) of the observed emission from the jet.

The effect on the energy flux for an approaching jet is given by :  $I_{obs} = I_{em} \delta^4$

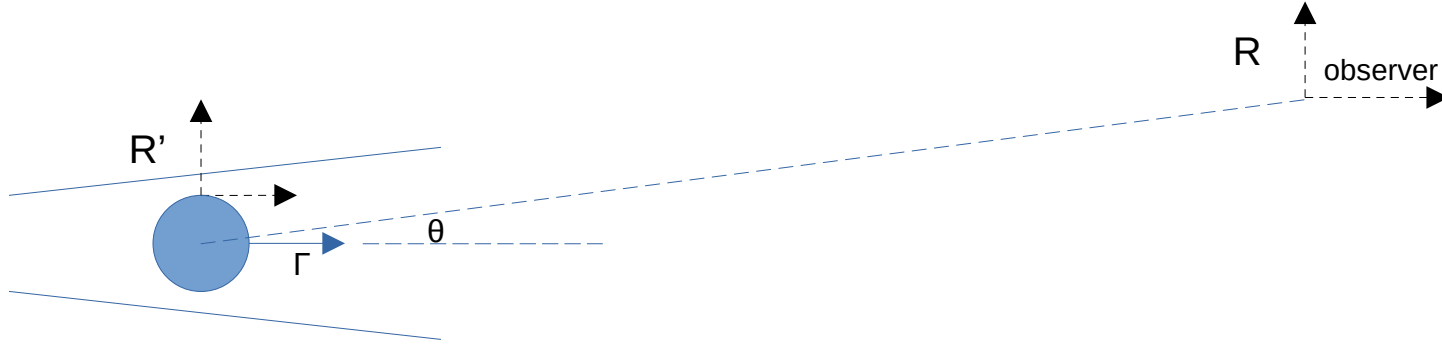
For typical Doppler factors of the order of 10, this leads to an amplification by a factor 10 000 !

The observed flux from the counter-jet is de-amplified by the same factor.

This explains why one often observes only a single jet !



# relativistic beaming explained



emitting region moving with Lorentz factor  $\Gamma = 1/\sqrt{1-\beta^2}$  along jet

- isotropic emission of light in comoving frame  $R'$

- emitted specific intensity  $I'_\nu(\nu')$

Doppler factor between  $R'$  and  $R$ :

$$\delta = \frac{1}{\Gamma(1-\beta \cos(\theta))}$$

observer frame  $R$  views jet axis under viewing angle  $\theta$

- observed specific intensity  $I_\nu(\nu)$

# relativistic beaming explained

Specific intensity is defined as  $I_\nu(\nu) = \frac{dE}{dt d\Omega dA d\nu}$  [ erg s<sup>-1</sup> cm<sup>-2</sup> sr<sup>-1</sup> Hz<sup>-1</sup> ] .

$I_\nu(\nu)/\nu^3 = I_{\nu'}(\nu')/\nu'^3$  is a Lorentz invariant ! (cf *Rybicki & Lightman*)

Thus :  $I_\nu(\nu) = I_{\nu'}(\nu') \left(\frac{\nu}{\nu'}\right)^3$  and  $\nu = \nu' \delta$

=>  $I_\nu(\nu) = I_{\nu'}(\nu') \delta^3$

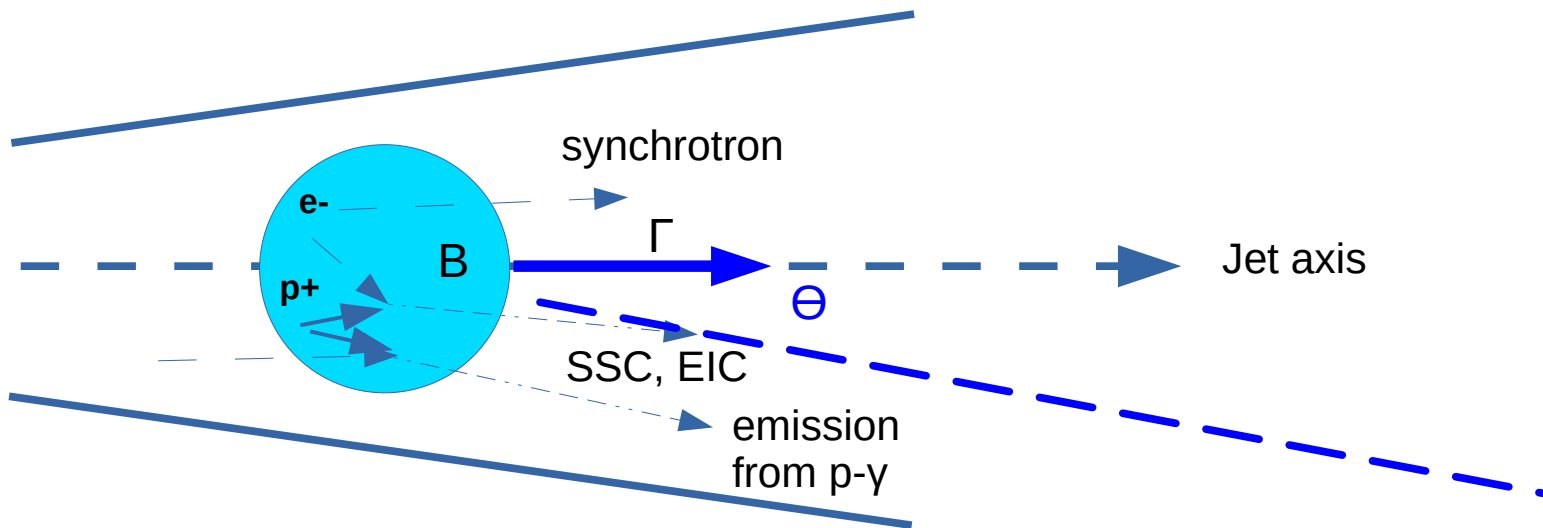
For the energy flux  $\frac{dE}{dt d\Omega dA}$  , this yields :  $\nu I_\nu(\nu) = \nu' I_{\nu'}(\nu') \delta^4$

If the specific intensity follows a power law :  $I_{\nu'}(\nu') = A (\nu')^{-\alpha} = A (\nu/\delta)^{-\alpha} = A \delta^\alpha (\nu)^{-\alpha}$

=>  $I_\nu(\nu) = \delta^{3+\alpha} I_{\nu'}(\nu')$

**attention:** The formulas above apply to emission from a discrete emission region inside the jet (“blob”). When describing the emission from the whole steady-state jet, the result changes, as discussed, for example, in the Appendix of *Sikora, M. et al. 1997*.

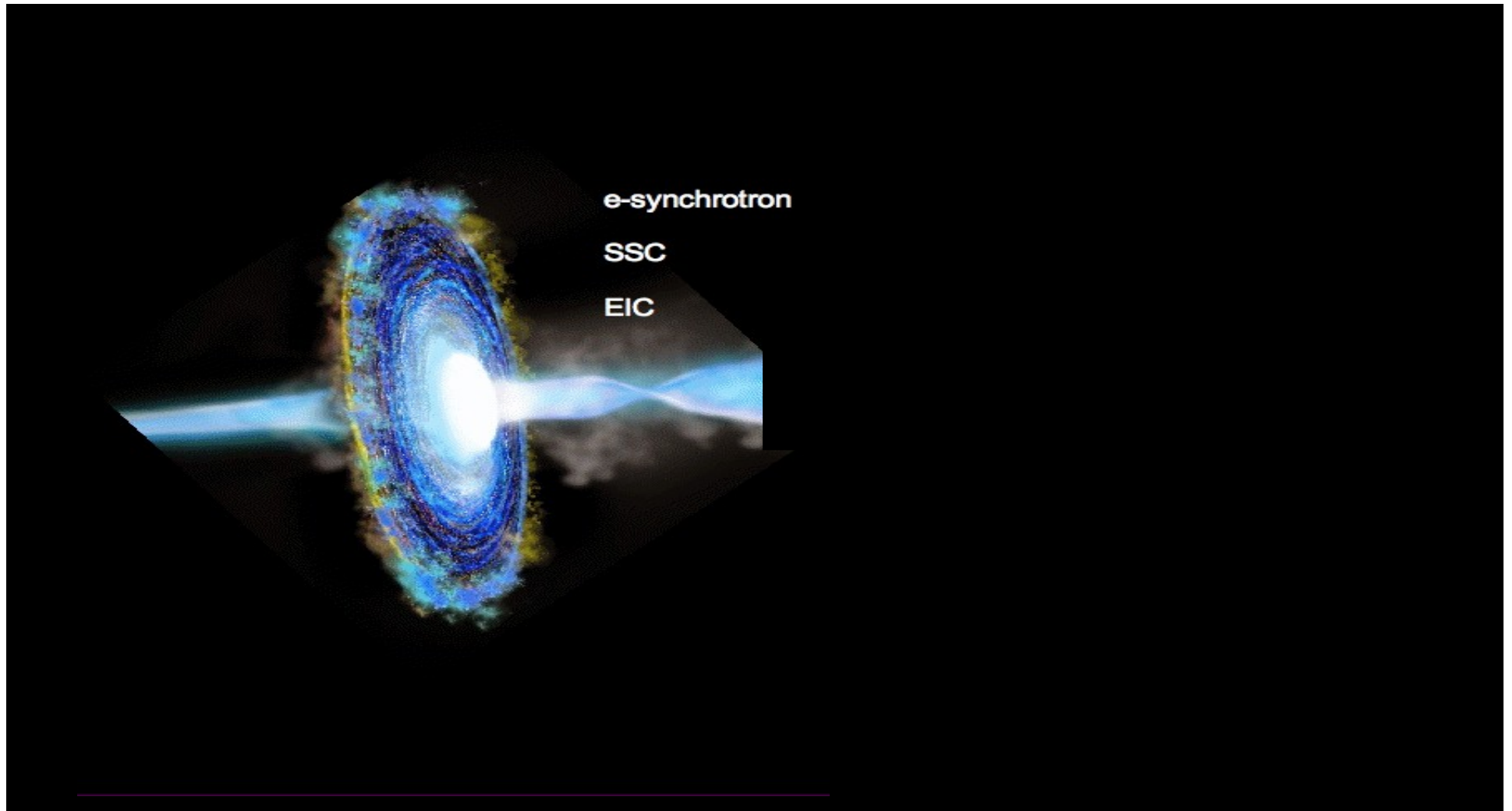
# blazar emission: one-zone models



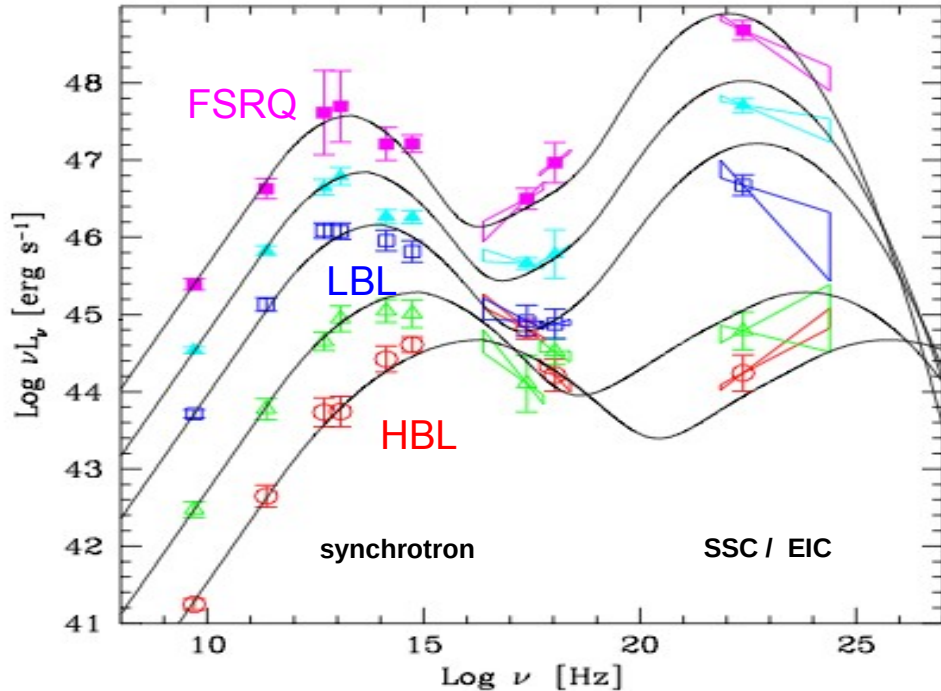
- plasma blob inside jet with turbulent magnetic field and high energy electrons / positrons (and protons)
- emission from radio to X-rays due to **synchrotron** radiation
- $\gamma$ -rays from **Synchrotron Self-Compton** or **External Inverse Compton** diffusion (on BLR or torus photons) or **interactions of protons** with magnetic or photon fields



# leptonic models

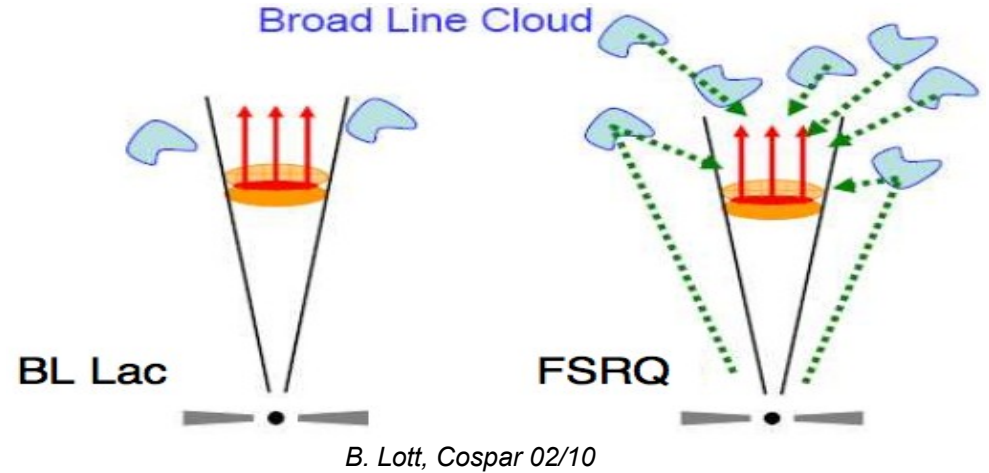


# blazar emission in the leptonic model



Donato et al. (2002), based on Fossati et al. (1998)

different blazar types : luminous FSRQs with high peaks in gamma band ↔ less luminous BL Lac objects with lower peaks in gamma band



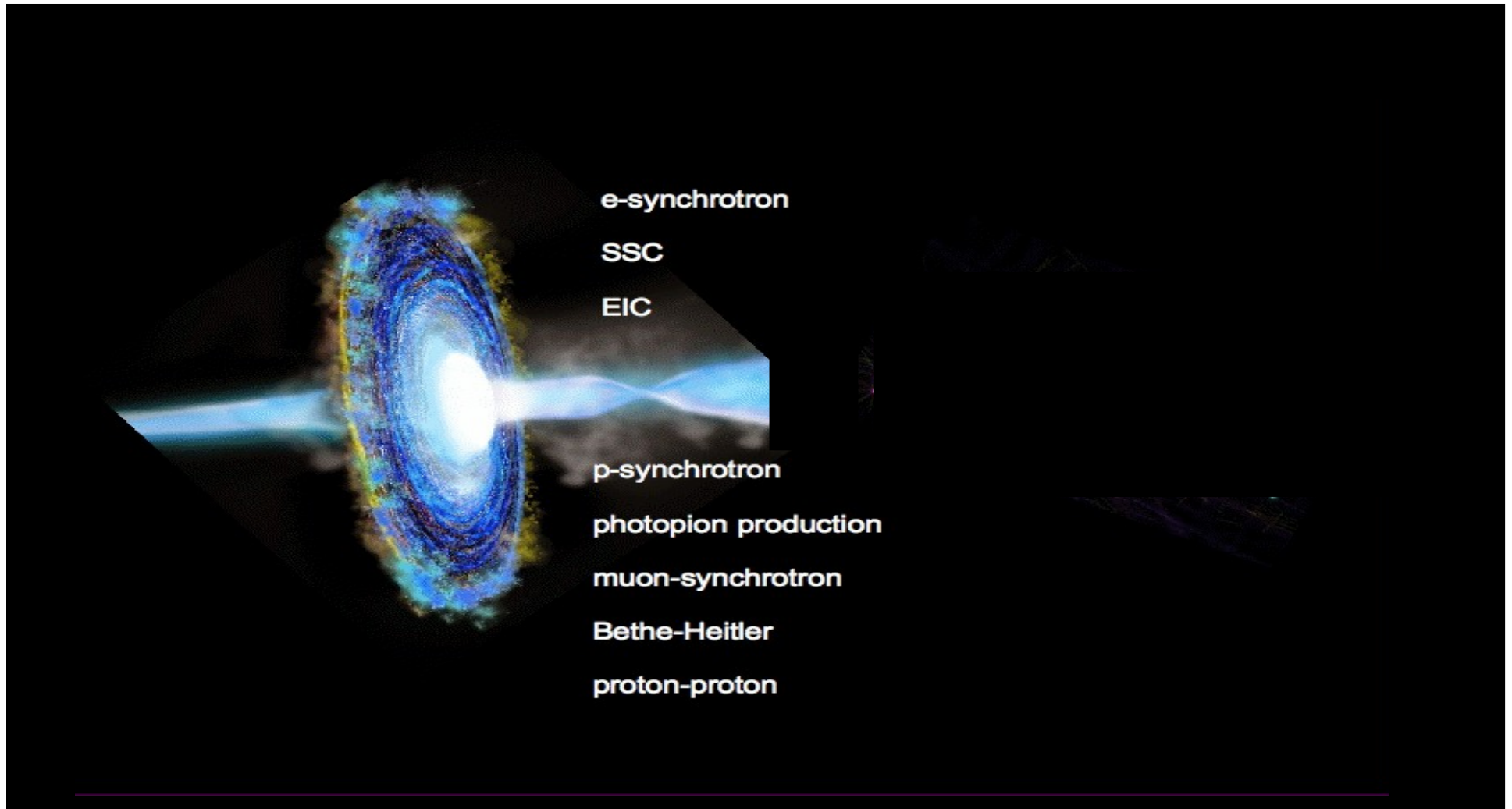
- Disk and Broad Line Region weak

-  $\gamma$ -rays due to Synchrotron Self Compton

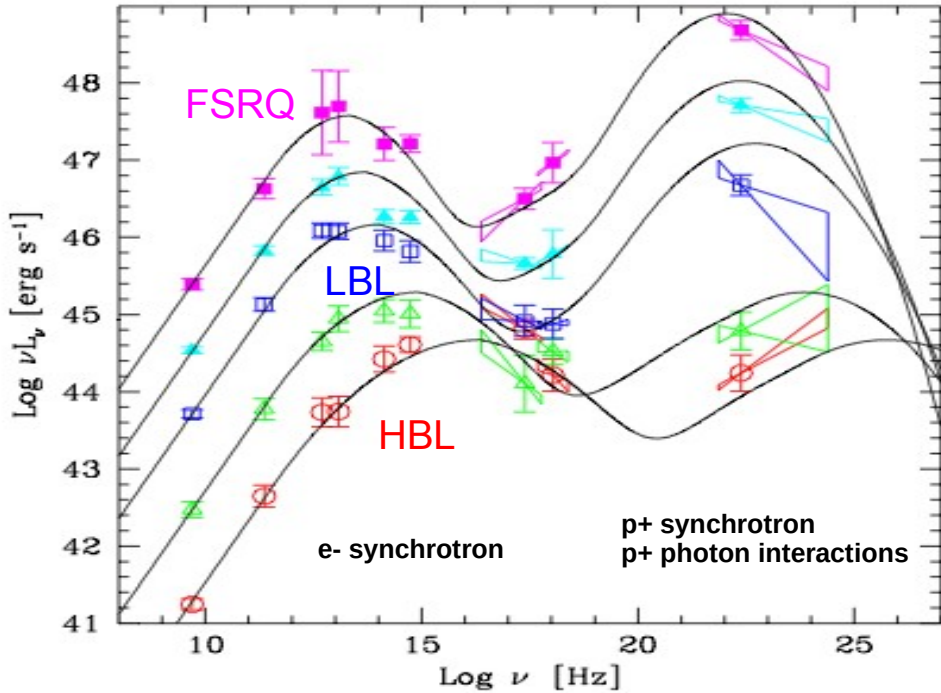
- Disk and Broad Line Region strong

-  $\gamma$ -rays due to Synchrotron Self Compton & External Inverse Compton  
→ high Compton dominance

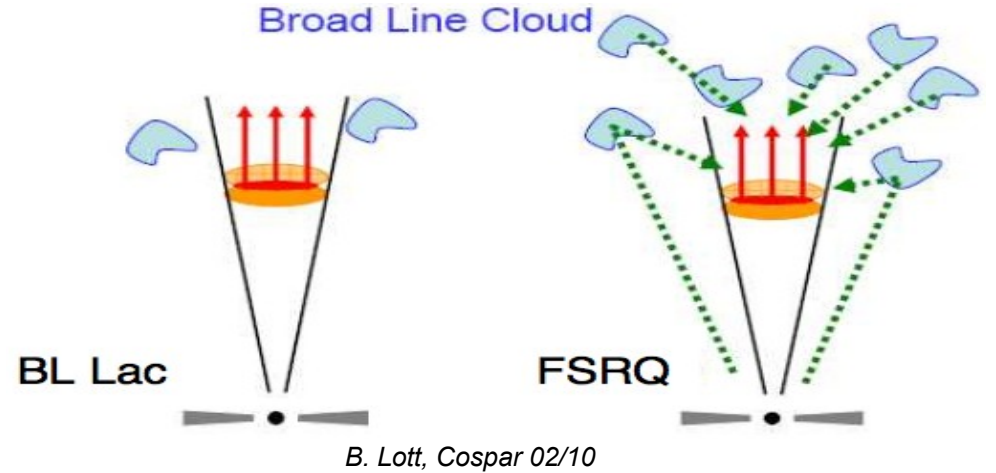
# lepto-hadronic models



# blazar emission in the lepto-hadronic model



Donato et al. (2002), based on Fossati et al. (1998)



B. Lott, Cospar 02/10

- Disk and Broad Line Region weak

-  $\gamma$ -rays due to mostly proton synchrotron emission ?

- Disk and Broad Line Region strong

-  $\gamma$ -rays due to proton synchrotron and proton-photon emission ?

# leptonic vs. lepto-hadronic models

## leptonic models :

low B-fields ( $\sim 0.01-1$  G)

+ rapid variability

+ jet power  $\ll L_{\text{edd}}$

- description of “orphan” gamma-ray flares difficult

- no link with multi-messengers

## hadronic models:

high B-fields ( $\sim 1-100$  G)

+ make the connection with neutrinos and cosmic rays

+ solutions for certain data sets, where leptonic models struggle

- require high jet powers ( $\sim L_{\text{edd}}$  or above)

- description of rapid flares difficult: longer acceleration and cooling time scales  
( factor  $(m_p / m_e)^4$  for synchrotron cooling at a given energy ! )

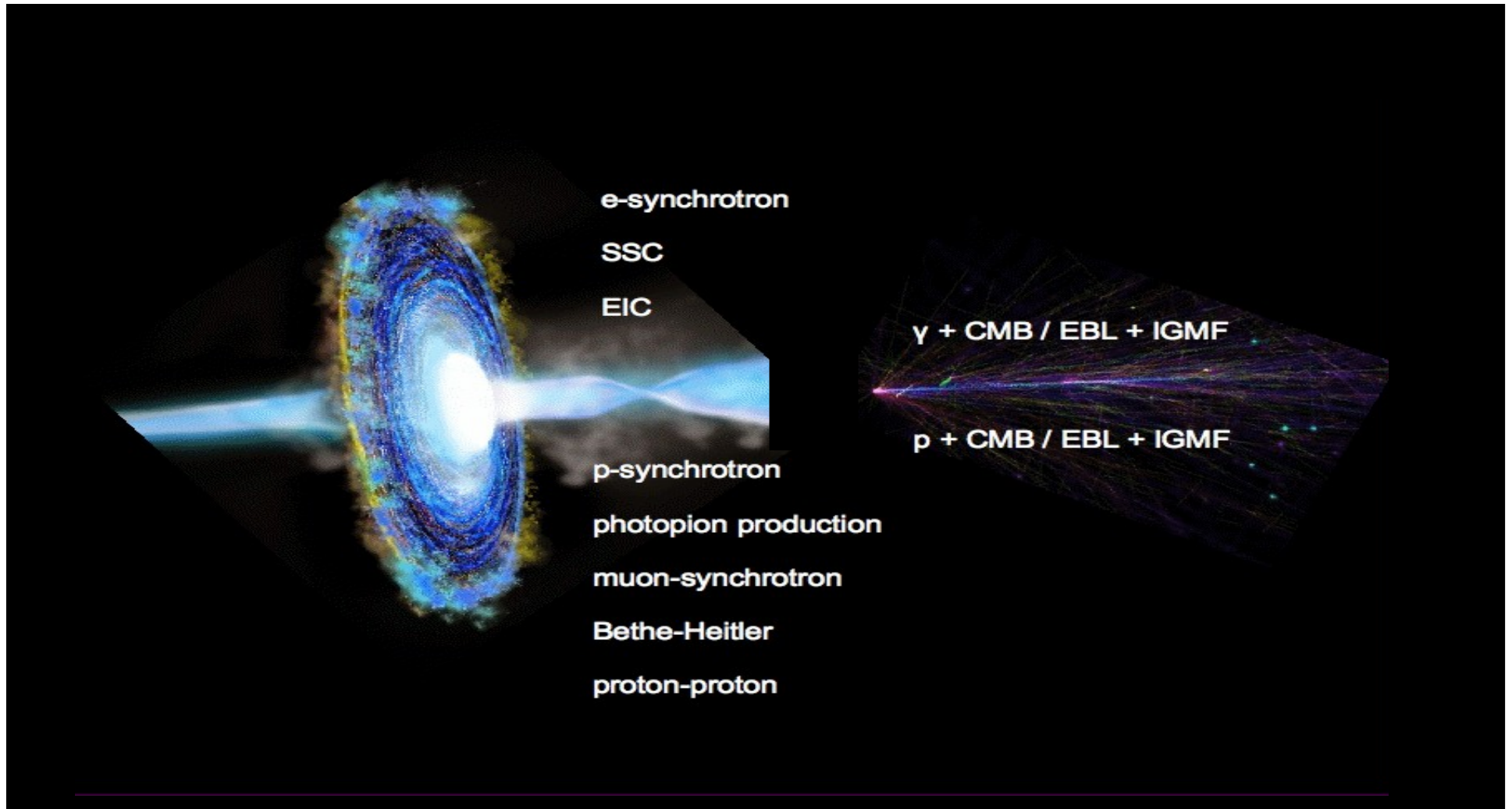
$$t_p \propto E_p / P_{\text{syn}_p} \propto \gamma_p m_p m_p^2 / \gamma_p^2 \propto m_p^3 / \gamma_p$$

$$E_p = E_e \rightarrow \gamma_p = \gamma_e \frac{m_e}{m_p}$$

$$\rightarrow \frac{t_p}{t_e} = \frac{m_p^3}{m_e^3} \frac{\gamma_e}{\gamma_p} = \frac{m_p^4}{m_e^4}$$



# lepto-hadronic models

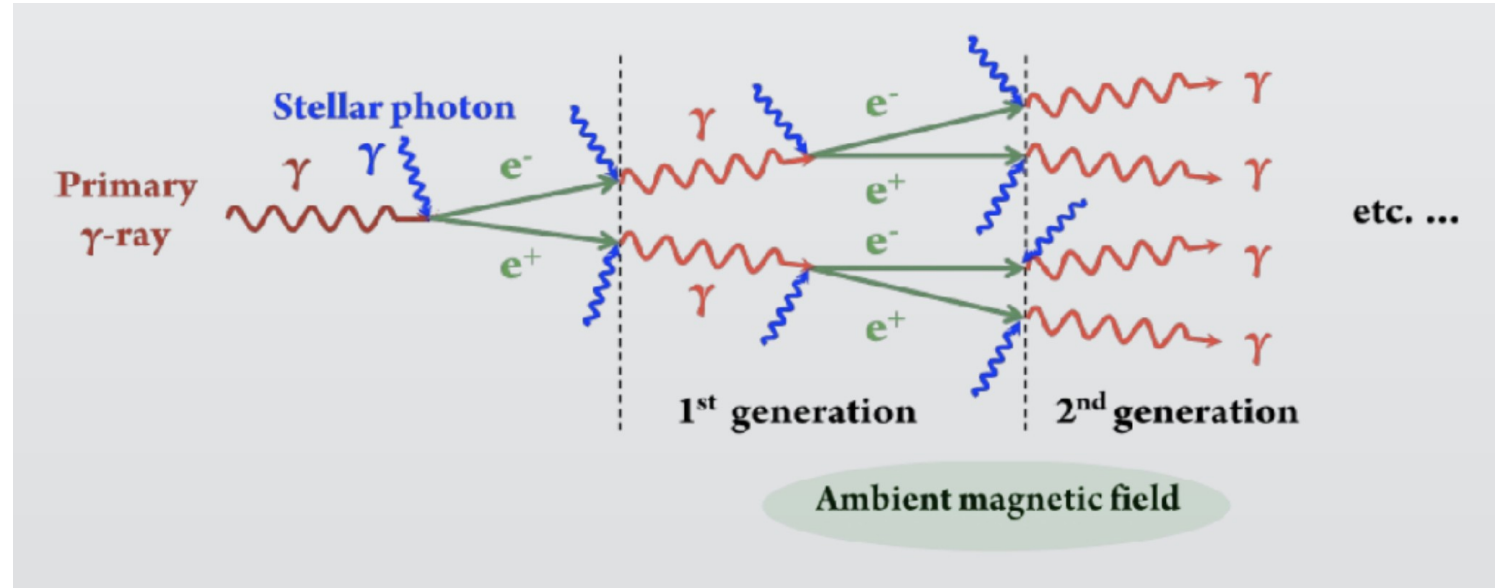


# reminder: pair cascades

In optically thick targets, the combination of pair production and a radiative process can lead to electromagnetic cascades that dissipate the energy of an initial high-energy particle.

examples :

- $\gamma$ -ray or  $e^-/e^+$  induced **synchrotron-pair cascade** in emission regions with strong B-fields and ambient photon fields



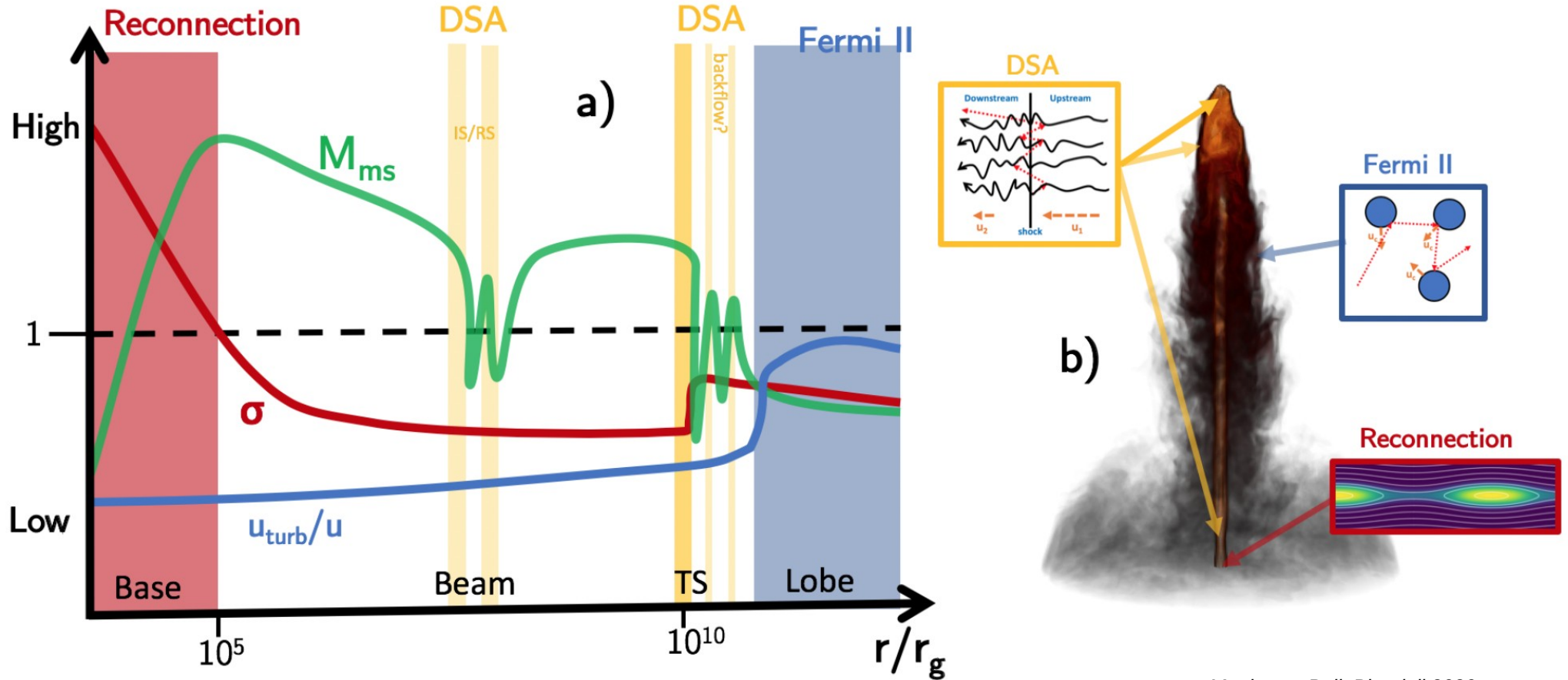
R.Belmont

- $\gamma$ -ray or  $e^-/e^+$  induced **IC – pair cascades** in the interstellar / intergalactic medium (upscattering of CMB / EBL / stellar photons and pair production)

- $\gamma$ -ray or  $e^-/e^+$  induced **electromagnetic air shower** (pair-production & bremsstrahlung in the atmosphere)

# particle acceleration in jets

Possibly there is no single mechanism at play, but several mechanisms contribute in different regions of the jet.



Matthews, Bell, Blundell 2020

# X-ray polarization

Detection of X-ray polarization is now possible thanks to the IXPE space telescope.

Observations of the blazar Mrk 501 (during a low state) show a **polarization degree that is increasing from the radio to optical to X-rays** and a **polarization angle aligned with the jet axis**.

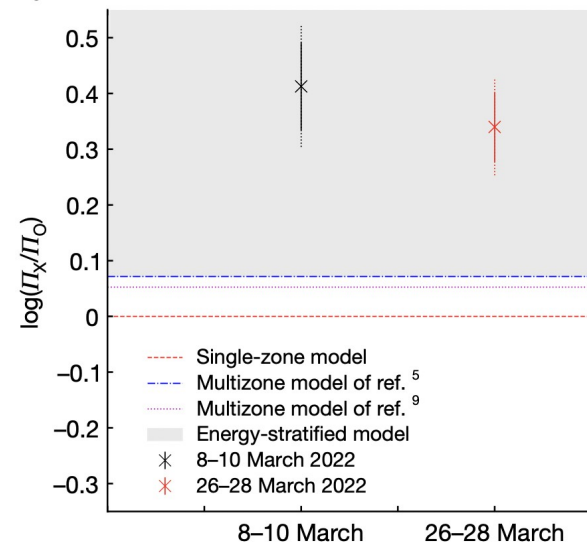
Interpretation through **shock acceleration** :

A shock partially orders the magnetic field of the plasma crossing it

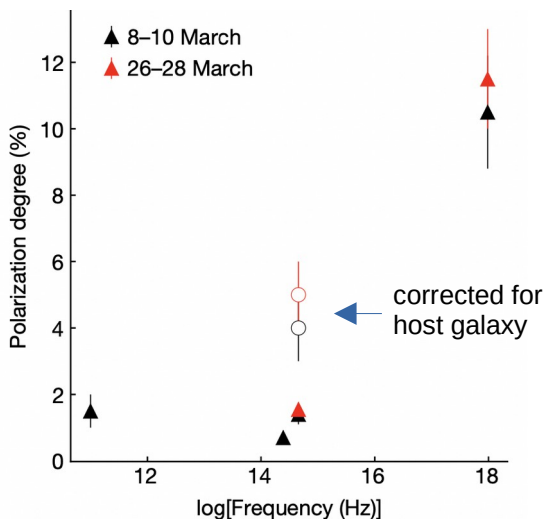
→ net polarization vector aligns with the jet

Particles accelerated on shock, progressively lose energy and emit at lower and lower frequencies as they diffuse away from the shock. Farther from the shock, the plasma becomes increasingly turbulent.

→ polarization decreases from high to low energy emission

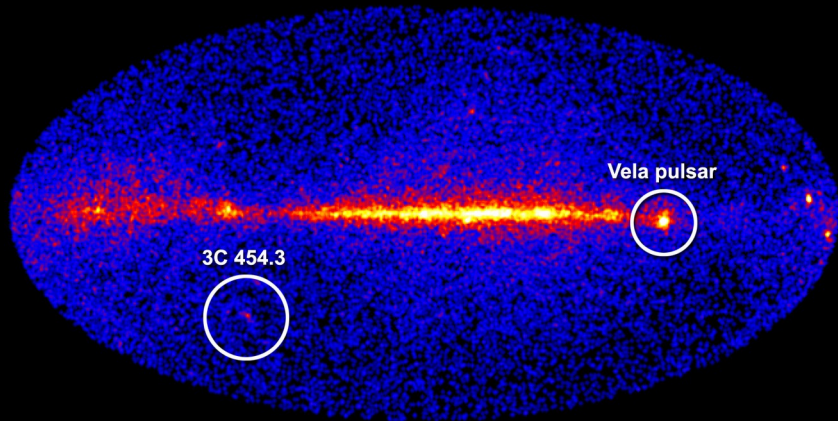


polarization ratio X-ray / optical compared to different emission models  
(Liodakis et al. 2022)

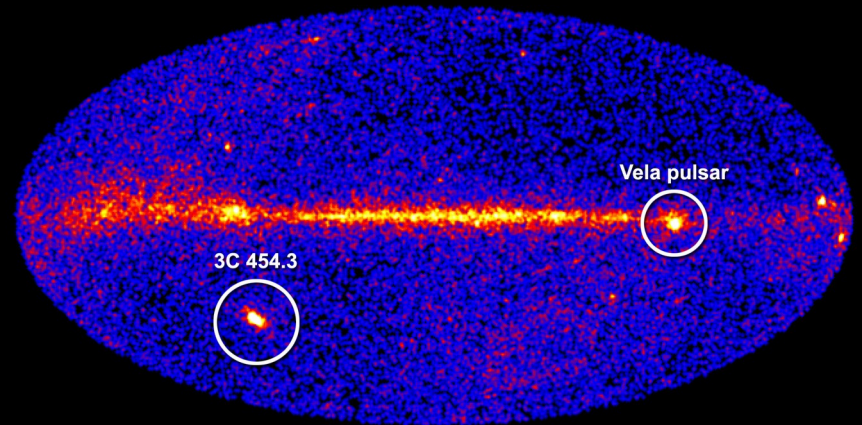


polarization from Mrk 501 from radio to X-rays  
(Liodakis et al. 2022)

### 3) rapid variability



November 3, 2009

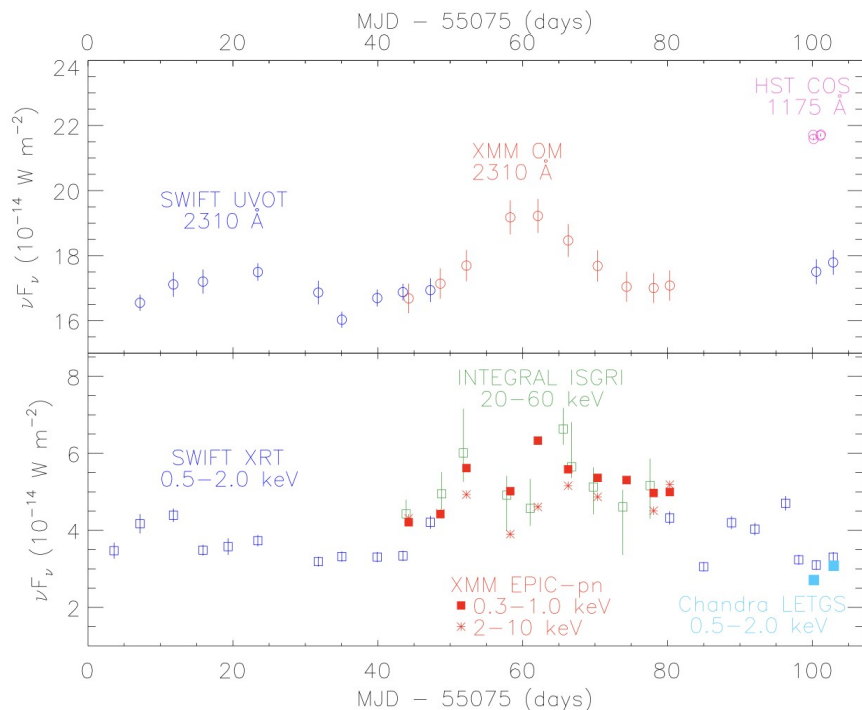


December 2, 2009

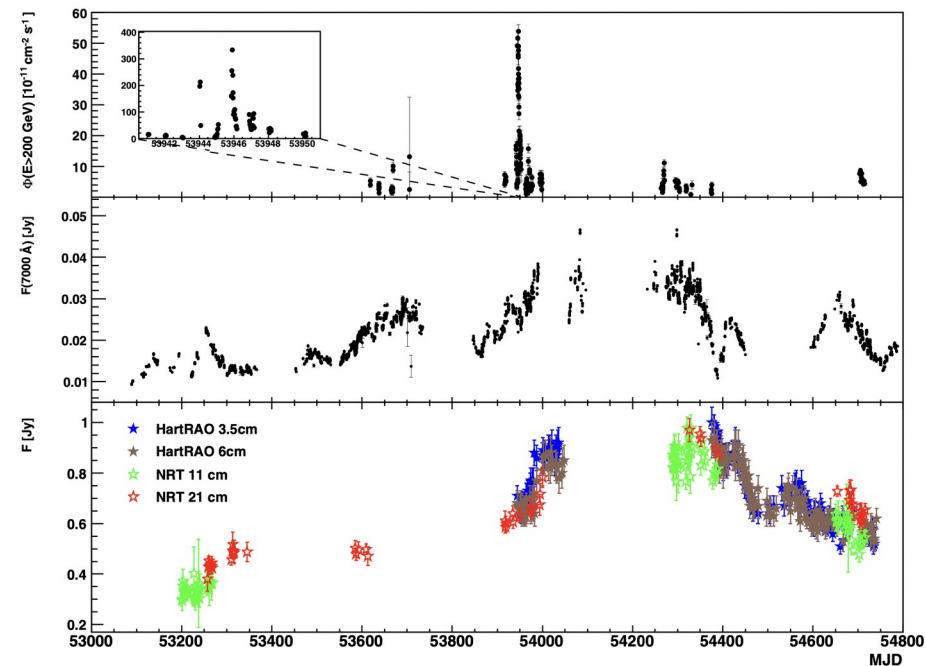
# AGN variability

Radio-loud and radio-quiet AGNs have shown **variability at all wavelengths**.

Variations are generally aperiodic (except for some cases of quasi-periodic oscillations) and have variable amplitude. The most rapid variability is observed at the shortest wavelengths.



UV and X-ray light curves of the **Seyfert 1** galaxy Mrk 509 (Kaastra et al. 2011)



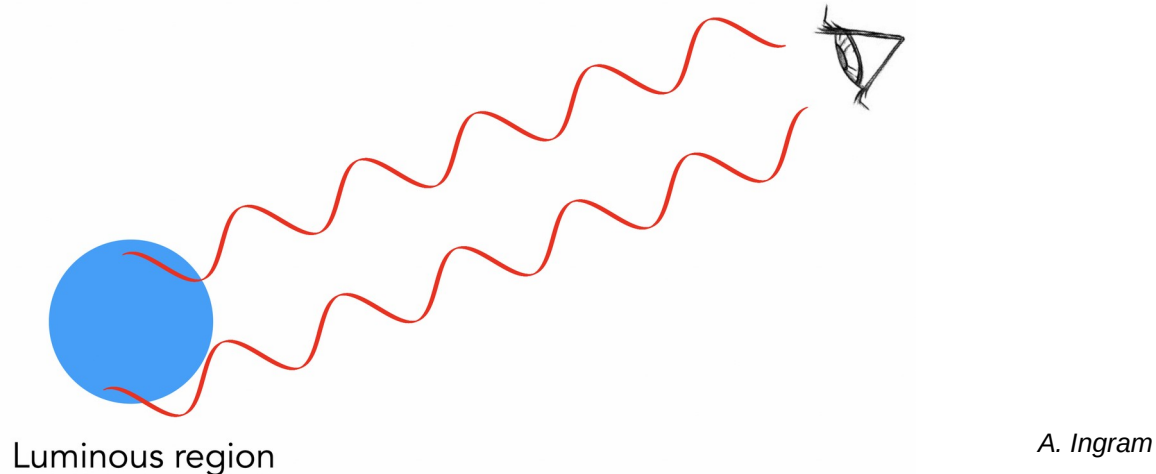
VHE, optical and radio light curves of the **blazar** PKS 2155-304 (HESS Collaboration 2012)

# rapid variability = compact emission region

Detection of rapid variability in quasars constrained the size of the emission region through the light travel time (or source coherence / causality) argument :

For a source to vary coherently in flux, the emission region must be causally connected, which implies a maximum size of  $R \leq c t_{\text{var}}$  for a typical variability time scale  $t_{\text{var}}$ . If this was not the case, stochastic variations from different source regions would average out.

→ Observation of day-scale variations in the optical band led to size constraints of a light day ( $\sim 3 \times 10^{15}$  cm) for the quasar emission region.



*A. Ingram*





# blazar flares

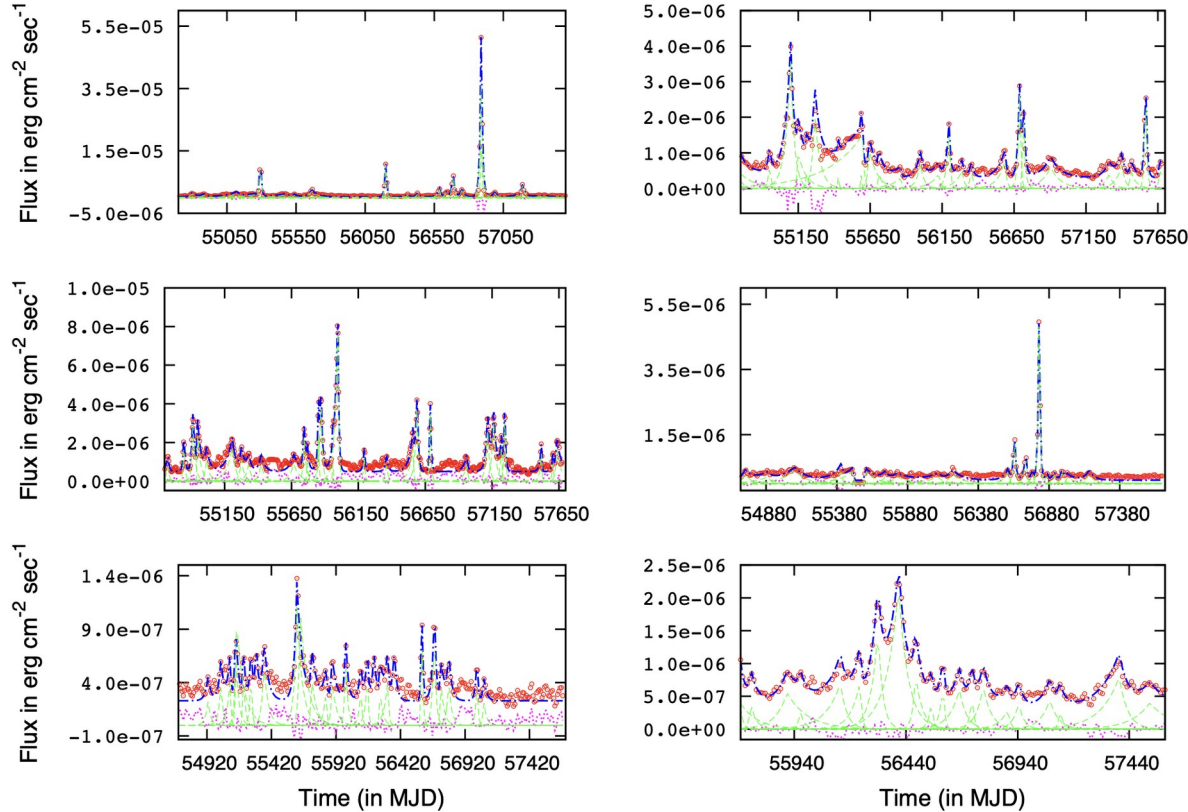


**Figure 1.** Top left – 3C 279; top right – 3C 273; middle left – 1510-089; middle right – Mrk 501; bottom left – PKS 2155-304; bottom right – PKS 1424-41. The red open circles denote the *Fermi*-LAT light curves of the above blazars at the energy range 0.1–300 GeV, which are smoothed with a Gaussian function of width 10 days; green long-dashed lines represent the individual decomposed flares (see the text), the blue dot-dashed line is the best fit to the model function given in Section 3.1, which is the sum of the individual flares, while the magenta dotted line is the residue after the fit.

Roy et al. 2019

Study of  $\sim 200$  long-term ( $\sim$ weeks–months) GeV and R-band outbursts and  $\sim 25$  short-term ( $\sim$ hour–day) GeV flares in a sample of 10 blazars from the *Fermi*-LAT and the Yale/SMARTS monitoring programme.

→ Most of the **long-term outbursts** are **symmetric**, indicating that the observed variability is dominated by the **crossing time-scale of a disturbance**.

→ A larger fraction of **short-term flares** are **asymmetric** with an approximately equal fraction of longer and shorter decay than rise time-scale.  
Signature of **gradual particle acceleration and cooling** ?

# origin of flares in the one-zone model

---

possible physical origin of flares :

- change in size of emission region  $R \rightarrow$  density  $n$ , magnetic field  $B$  (expansion, contraction)
- change in magnetic field  $B$
- change in Doppler beaming (Lorentz factor, viewing angle)
- particle injection (pre-accelerated particle distribution)
- particle acceleration (shock, turbulence, shear, magnetic reconnection)

# origin of flares in the one-zone model

electron evolution: 
$$\frac{\partial N_e}{\partial t} = \frac{\partial}{\partial \gamma} [(\beta \gamma^2 - 2D_0 \gamma - a \gamma + b \gamma) N_e] + \frac{\partial}{\partial \gamma} \left( D_0 \gamma^2 \frac{\partial N_e}{\partial \gamma} \right) - \frac{N_e}{t_{esc}} - \frac{N_e}{t_{ad}} + Q_{inj}$$
 Fokker-Planck equation

$Q_{inj}(\gamma, t)$  particle injection rate ,  $-\frac{N_e}{t_{esc}}$  particle escape rate,  $-\frac{N_e}{t_{ad}}$  adiabatic expansion rate

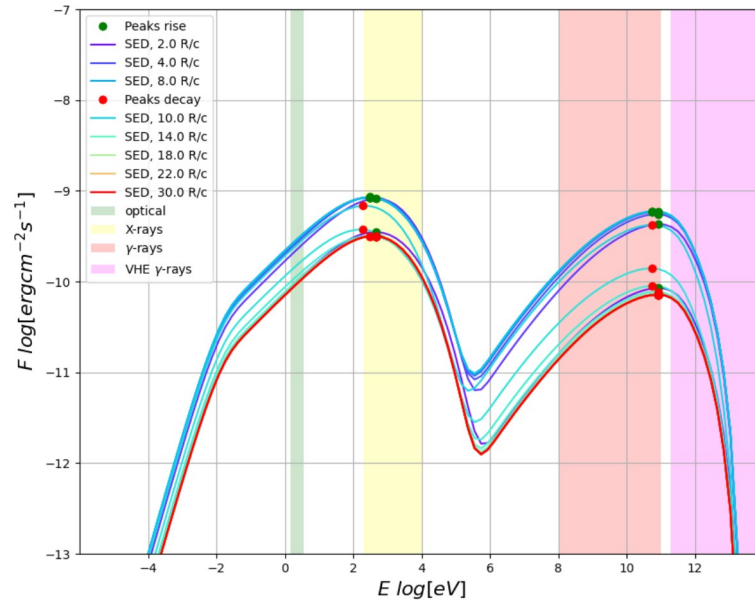
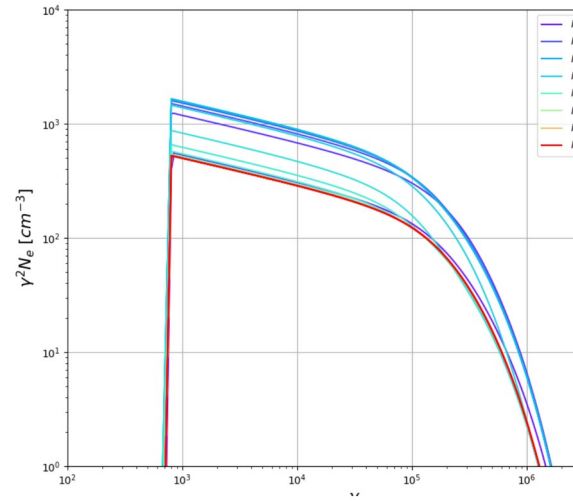
acceleration terms :

- Fermi I :  $a = 1/t_{shock}$  with  $t_{shock}$  the acceleration time scale
- Fermi II :  $D_0 = 1/t_{turb}$  with  $t_{turb}$  the acceleration time scale

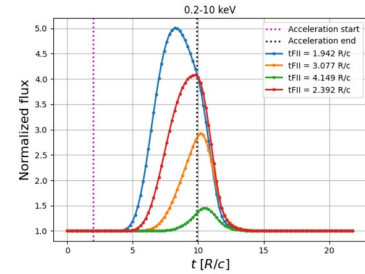
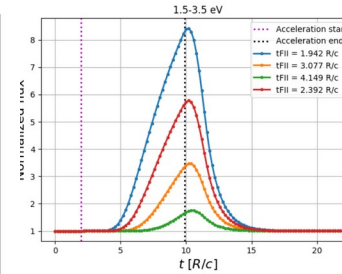
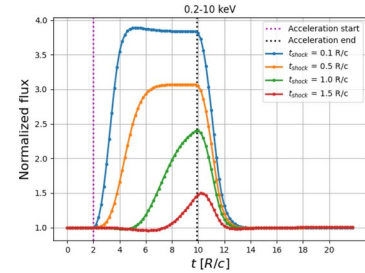
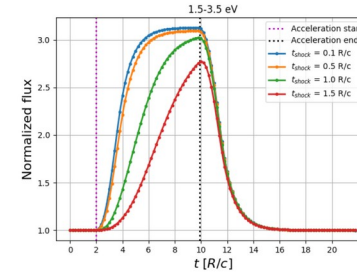
cooling terms :

- adiabatic  $\dot{\gamma}_{ad}(t) = \frac{\dot{V}}{3V} \gamma = \frac{\dot{R}(t)}{R(t)} \gamma = \frac{\beta_{exp} c}{R(t)} \gamma = b \gamma$
  - synchrotron  $\dot{\gamma}_{synch}(t) = \frac{4 \sigma_T c}{3 m_e c^2} \gamma^2 U_B(t)$  with  $U_B = \frac{B^2}{8 \pi}$
  - Inverse Compton (Thomson regime)  $\dot{\gamma}_{IC}(t) = \frac{4 \sigma_T c}{3 m_e c^2} \gamma^2 U_{ph}(t)$  with  $U_{ph}$  the (target) photon energy density
- }  $\beta \gamma^2$

# origin of flares in the one-zone model



Spectral Energy Distribution



Light curves  
(top: Fermi-I  
bottom: Fermi-II)

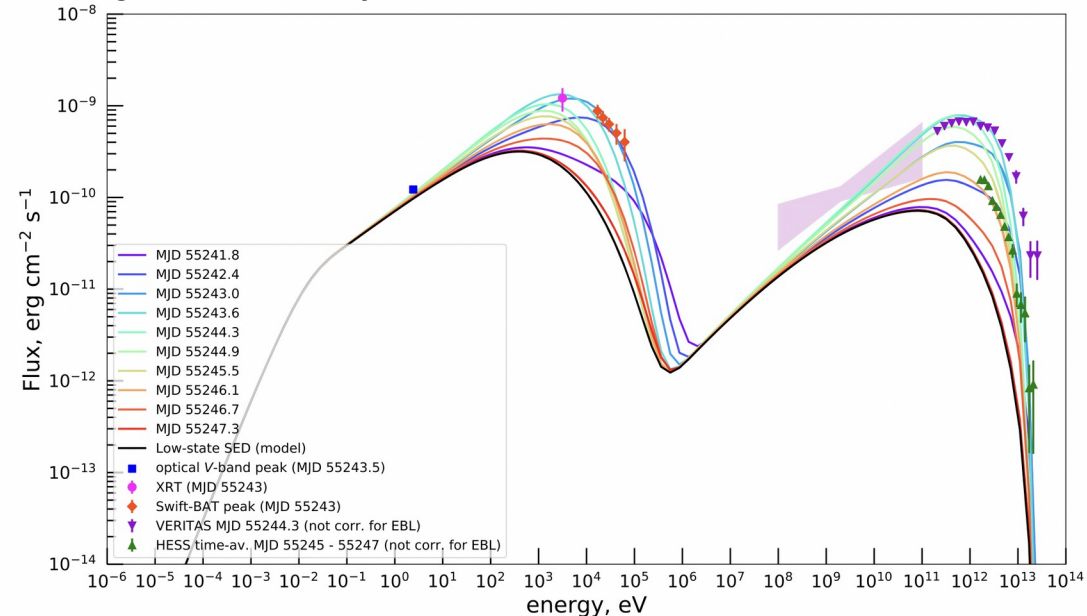
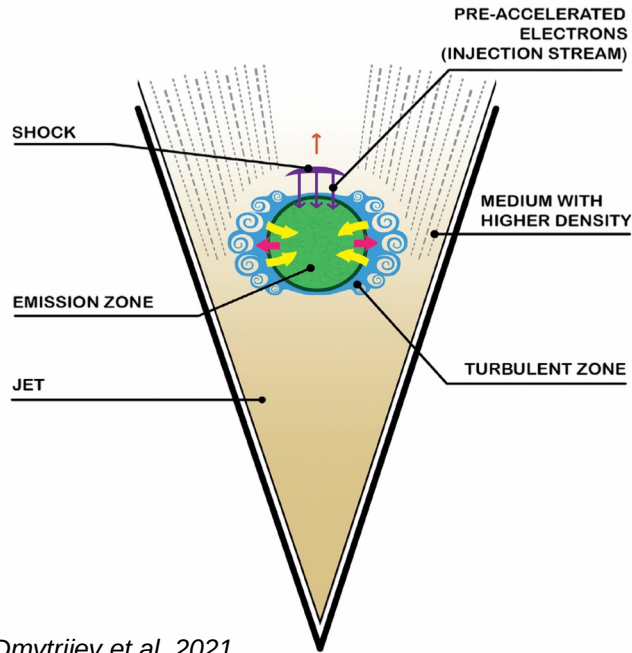
*P. Thevenet et al.  
Gamma 2024*

**e- distribution** : steady state (violet) + injection, radiative cooling, escape

# an example : modelling a flare from Mrk 421

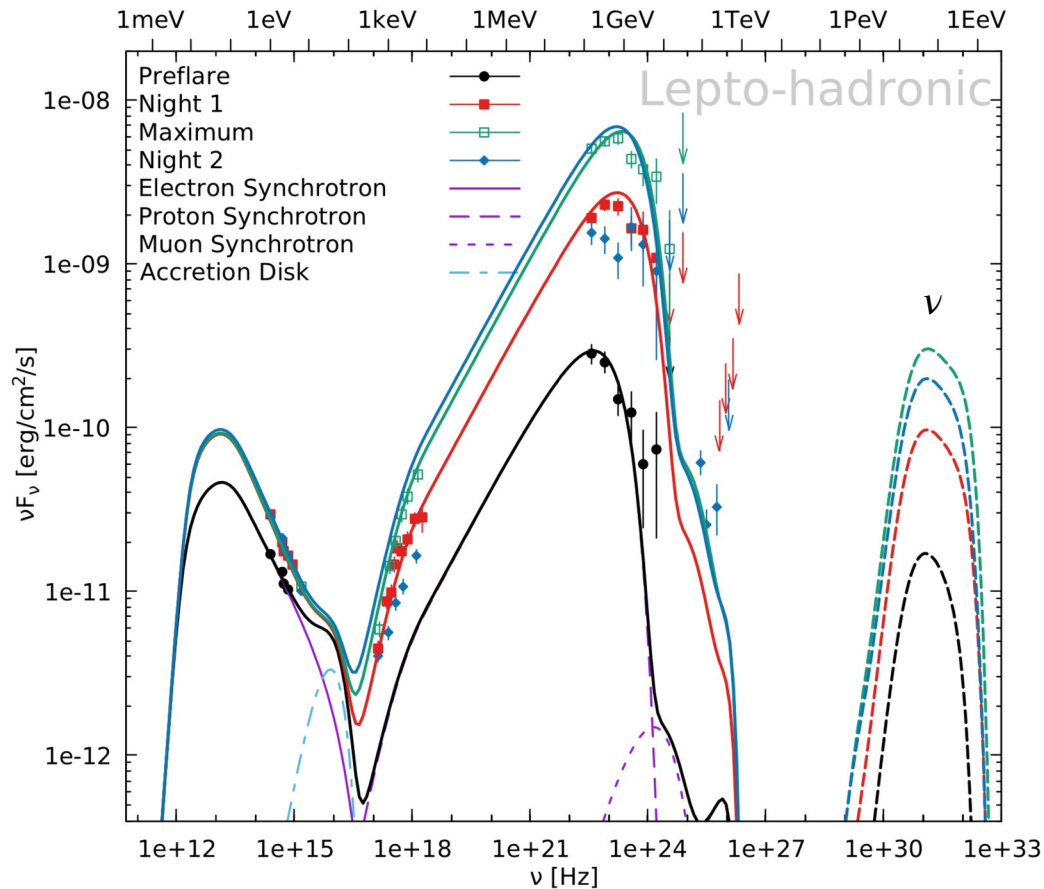
In this model, the continuous low-state emission from Mrk 421 is connected with a flare in Feb. 2010 :

- low state is modelled with a continuous injection (+ cooling, escape) of electrons accelerated on a (bow) shock into the emitting blob
- the hard spectrum during the flare requires additional Fermi II acceleration from a turbulent emission region surrounding the blob as it passes through an inhomogeneous region inside the jet.



Broad-band emission from Mrk 421 during low state and flare + model curves. (A. Dmytriiev et al. 2021)

# lepto-hadronic one-zone models



Model for a flare from the blazar 3C 279 in 2015  
(HESS Collaboration 2019)

- 3C 279 is a bright FSRQ-type blazar  
-> important photon fields

- $\gamma$ -ray emission region is at a distance  
> 0.06 pc from the central black hole,  
i.e. beyond BLR

- attempts to model this flare with one-zone  
leptonic or lepto-hadronic models are not  
entirely satisfactory...

- predicted number of  $\nu$  detectable with IceCube  
during flare very small ( $\sim 5 \times 10^{-4}$ )

# open-access codes to model AGN emission

Various open-source packages exist to model the broad-band emission of extragalactic sources from radio up to the highest gamma ray energies.

software	sources	approach	particles			processes						temp. ev.	emission region
			thermal	non-thermal e <sup>±</sup>   p		synch.	leptonic SSC   EC		Brems.	hadronic pp	absorption γγ		
naima	PWN, SNR, GRB	numerical	✗	✓	✓	✓	✓	✓(CMB)	✓	✓ <sup>†</sup>	✓(EBL)	✗	not specified
GAMERA	PWN, SNR, AGN microquasars	numerical	✗	✓	✓	✓	✓	✓ <sup>⊙</sup>	✓	✓ <sup>†</sup>	✓ <sup>*</sup>	✓ (only cool.)	multiple uniform
JetSeT	jetted AGN, PWN microquasars, SNR	numerical	✗	✓	✓	✓	✓	✓	✓	✓ <sup>‡</sup>	✓(EBL)	✓ (acc. + cool.)	multiple uniform acc. + rad.
agnpy	jetted AGN	numerical	✗	✓	✗	✓	✓	✓ <sup>*</sup>	✗	✗	✓ <sup>*</sup>	✗	single uniform
BHJet	binaries, AGN	numerical semi-analytical	✓	✓	✗	✓	✓	✓	✗	✗	✗	✗	whole jet
FLAREMODEL	synch. sources	numerical ray-tracing	✓	✓	✗	✓	✓	✗	✗	✗	✗	✓ (only cool.)	single radial dep.

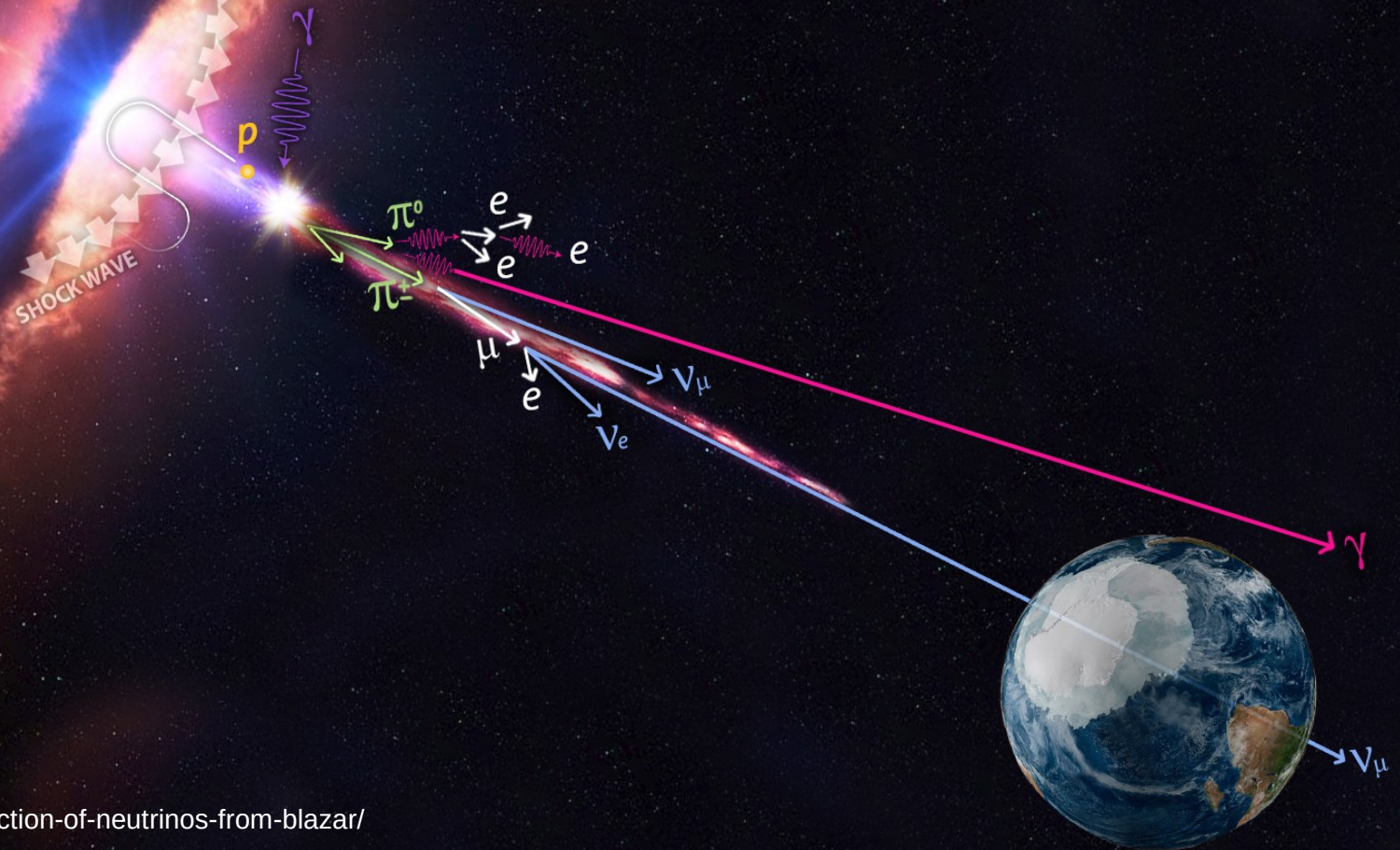
<sup>†</sup> pp interaction: computing only gammas from  $\pi_0$  decay.

<sup>‡</sup> pp interaction: computation of radiation from secondaries of charged pions (pairs evolved in time to equilibrium) and of  $\nu$  spectra.

<sup>⊙</sup> full angular dependency of the Compton cross section: anisotropic electrons and anisotropic photon fields.

<sup>\*</sup> full angular dependency of the Compton or  $\gamma\gamma$  cross sections: anisotropic photon fields.

## 4) AGN flares and neutrinos



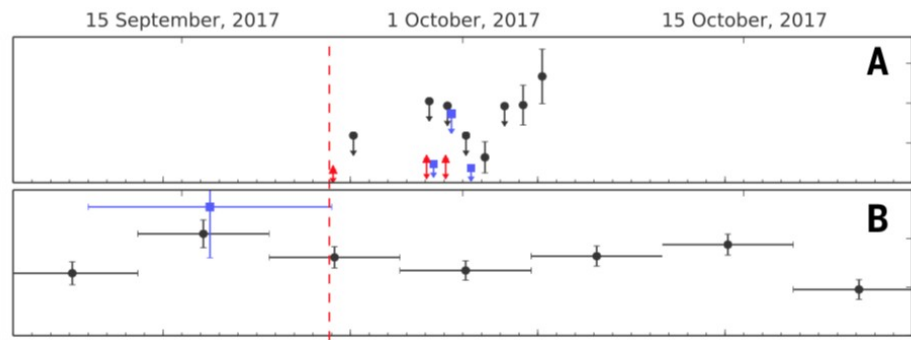
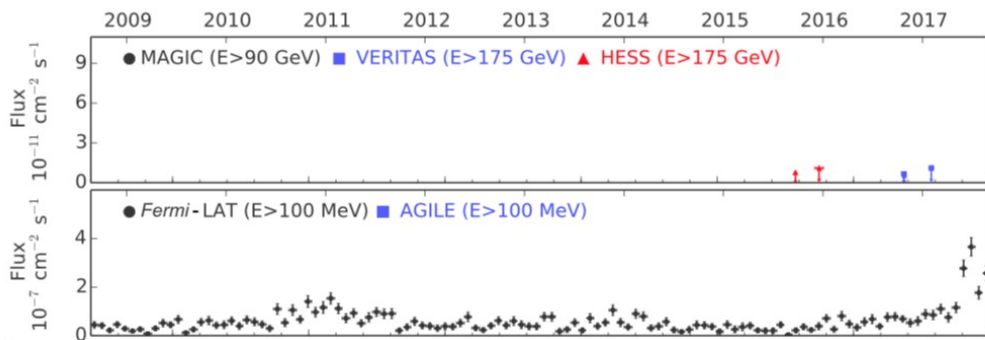
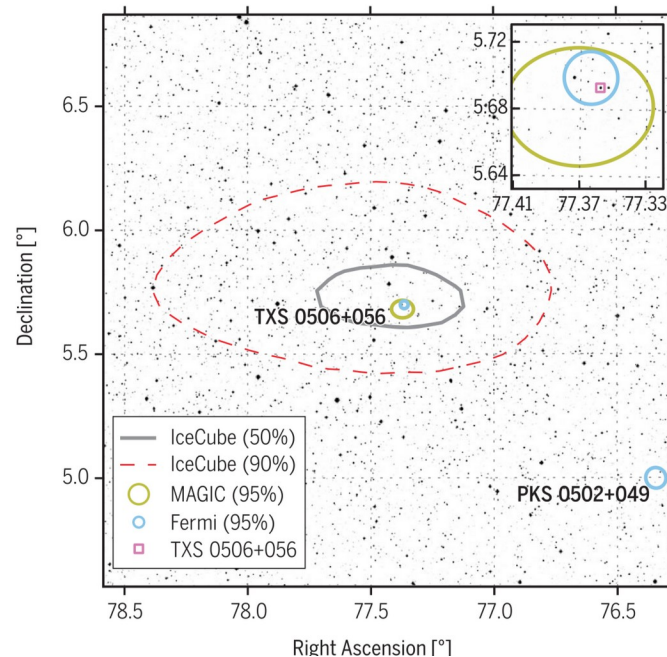


# TXS 0506+056: first extragalactic neutrino source?

First detection of a high-energy neutrino ( $\sim 290$  TeV) with IceCube from a known blazar during a  $\gamma$ -ray outburst (duration  $\sim 6$  months) in 2017, followed by a VHE flare seen with MAGIC.

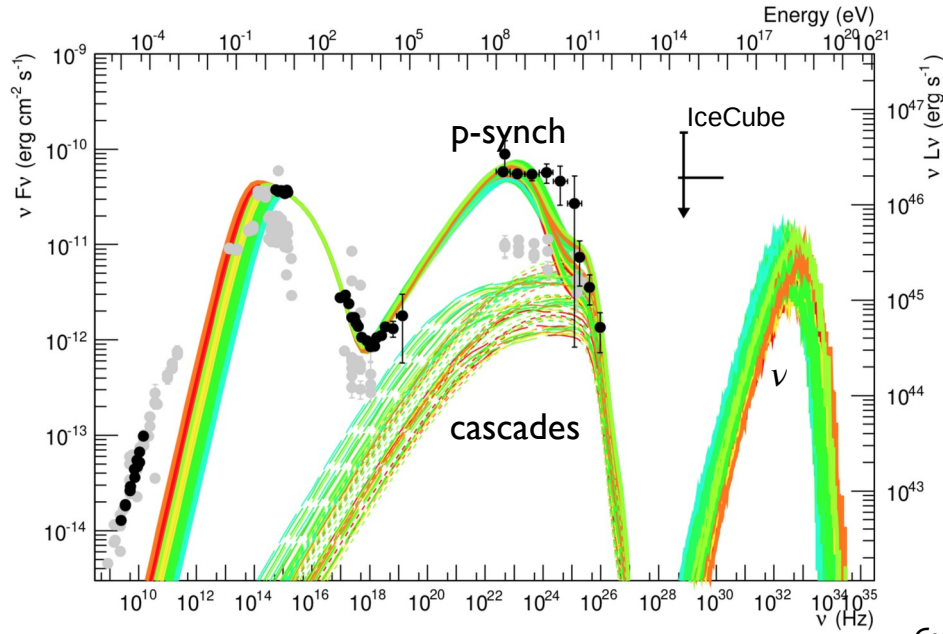
-> chance coincidence excluded at  $3\sigma$  level

Later also detection with the VERITAS Cherenkov telescopes.



Aartsen et al. 2018

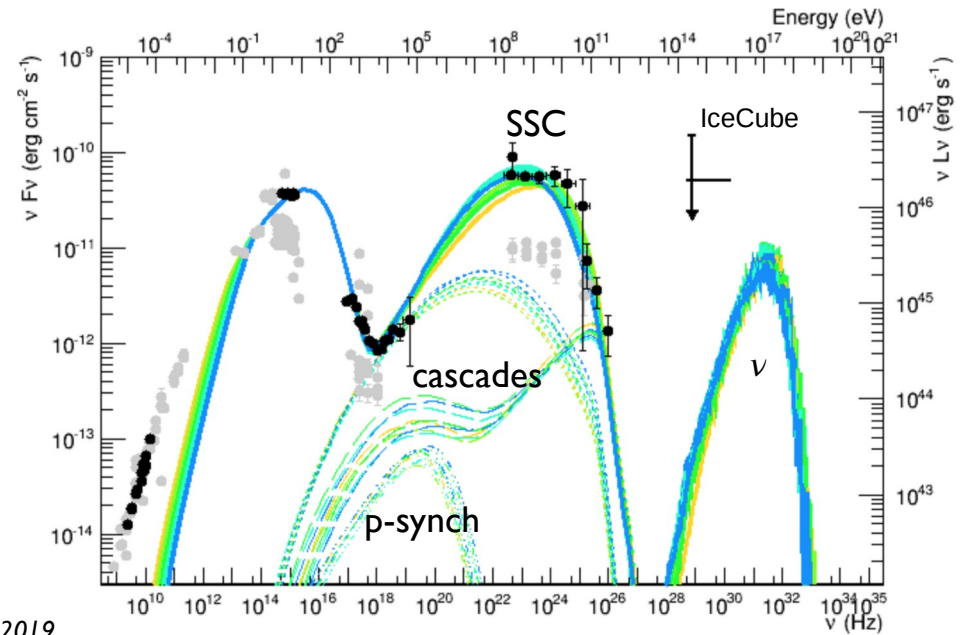
# interpretation with one-zone lepto-hadronic code



(a) Proton synchrotron modeling of TXS 0506+056

$\gamma$ -rays mostly p-synchrotron  
+ cascade emission

->  $\nu$  rate too low to be consistent with IceCube



(b) Lepto-hadronic modeling of TXS 0506+056

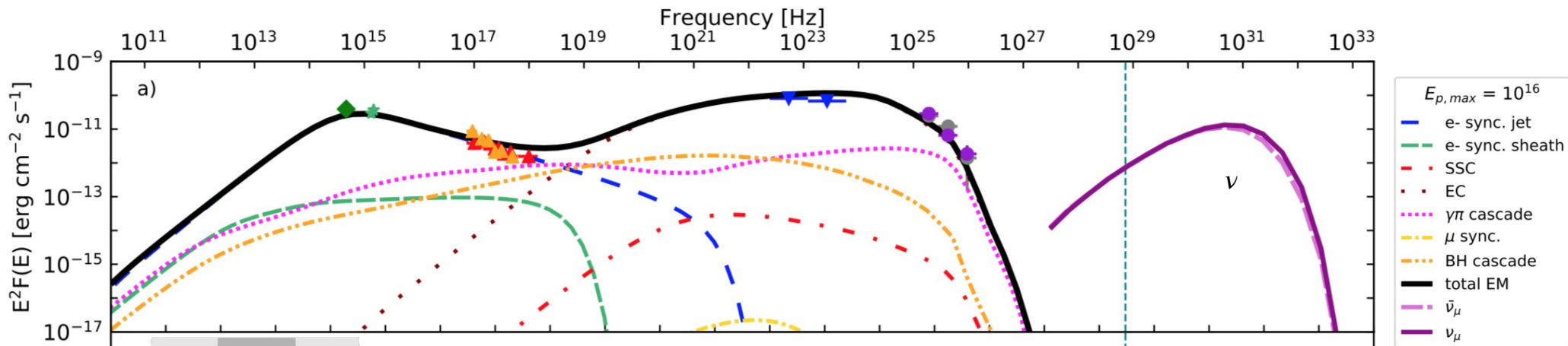
$\gamma$ -rays mostly SSC + cascade emission

->  $\nu$  flux marginally consistent with IceCube (prob. ~2%)

-> very high jet power

# external photon fields ?

e.g. *Ansoldi et al. 2018*: interactions of e- and p+ co-accelerated in the jet with external photons originating from a **slow-moving plasma sheath surrounding the faster jet spine**.

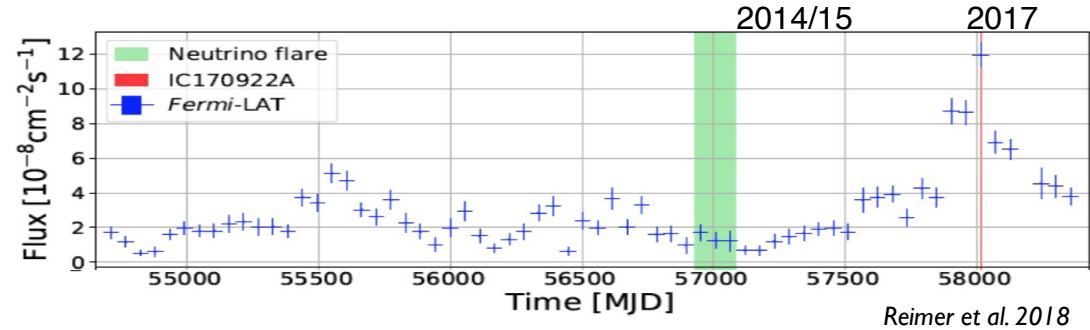
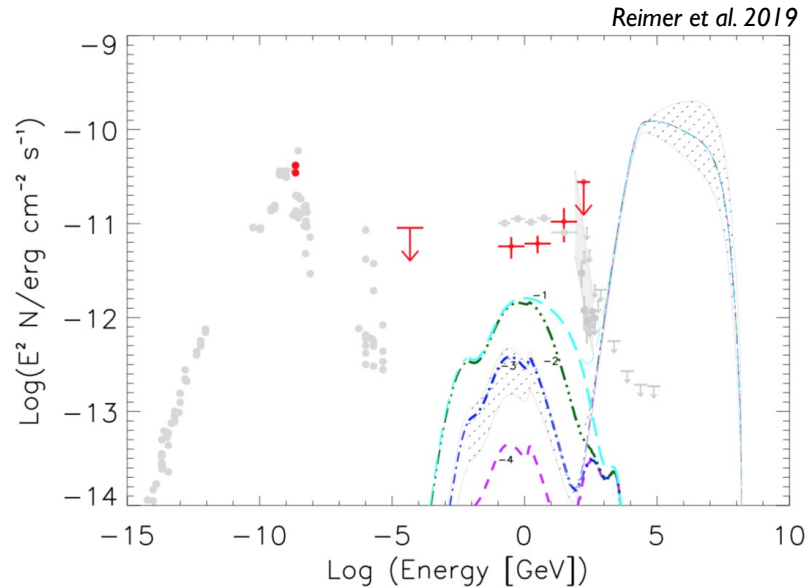


-> Good reproduction of MWL SED and neutrino rate (~0.2 events for flare), with acceptable jet power.

->  $\gamma$ -rays mostly from Inverse Compton up-scattering of the external ("layer") field.

# the 2014/15 “orphan” neutrino flare

Archival searches in IceCube then found a flare in the 2014/15 data ( $\sim 3.5\sigma$ ), not accompanied by any  $\gamma$ -ray flaring.

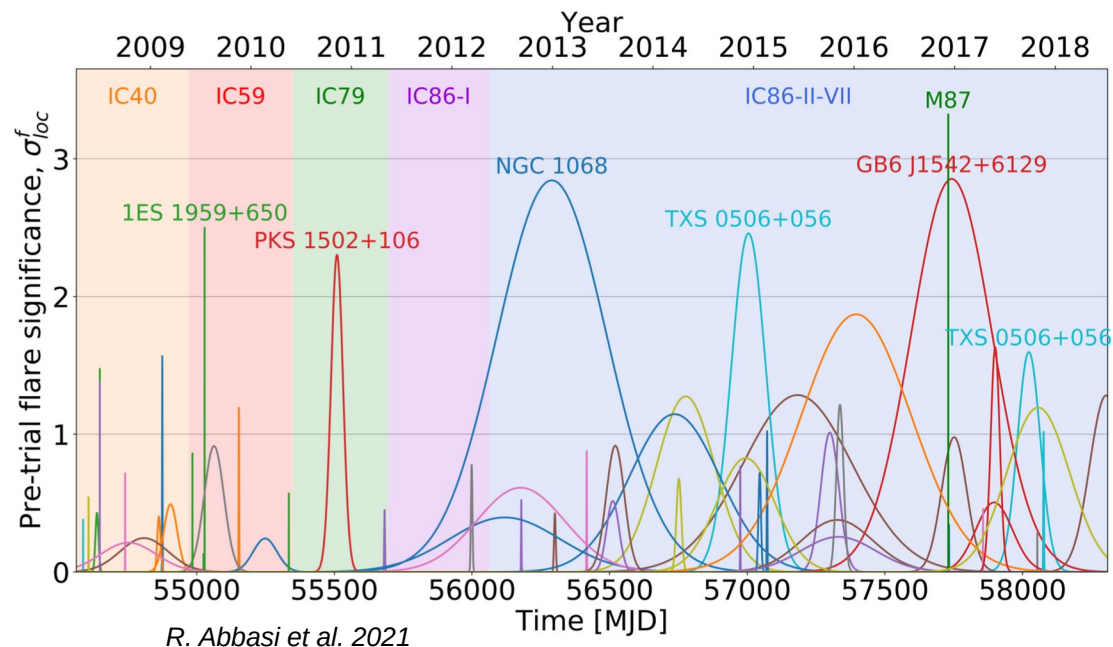


-> expect no direct connection between  $\gamma$ -ray flares and neutrino events

Only solution to explain  $\nu$  flare implies that the majority of  $\gamma$ -rays are emitted from another region in the source !

# neutrinos correlated with AGN flares ?

Search for time-dependent correlations between 10 years of IceCube data and a pre-defined catalog of 110 neutrino candidate sources.

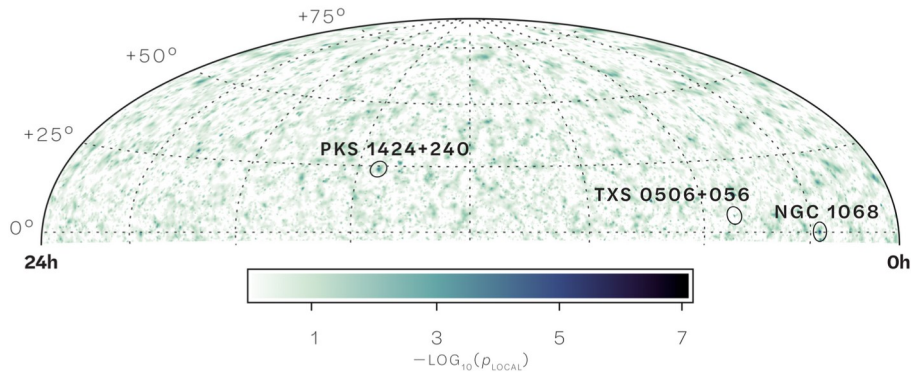


- Time-dependent statistical test of the Northern hemisphere suggests an incompatibility at **3.0  $\sigma$  significance** of the neutrino events from **four sources** with respect to the overall Northern background expectation :  
NGC 1068 (Seyfert2 & starburst) , TXS 0506+056 (blazar), GB6 J1542+6129 (blazar), M87 (radio-galaxy)

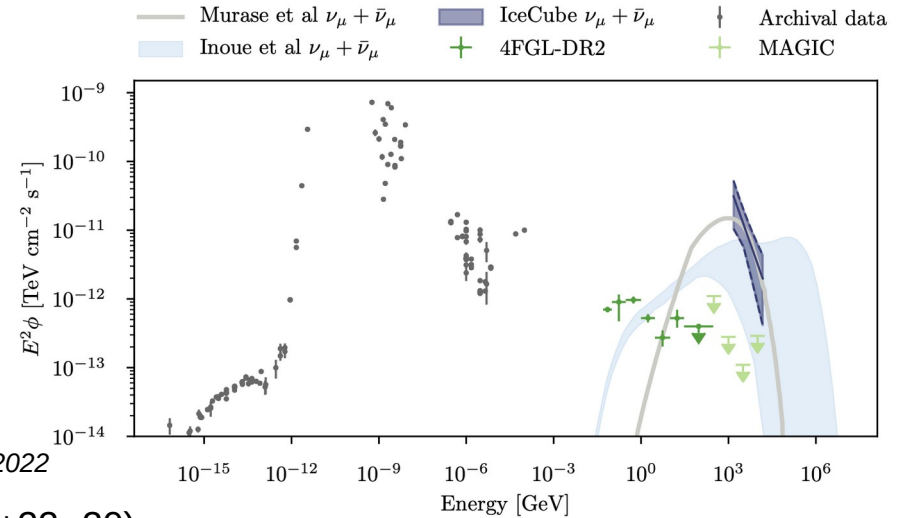
- The three first sources are also seen in time-independent studies, but not M87.

- No significant result in the Southern hemisphere  $\rightarrow$  consistent with the lower sensitivity due to the substantially larger background of atmospheric muons in the Southern hemisphere.

# neutrinos from NGC 1068



IceCube Collaboration 2022



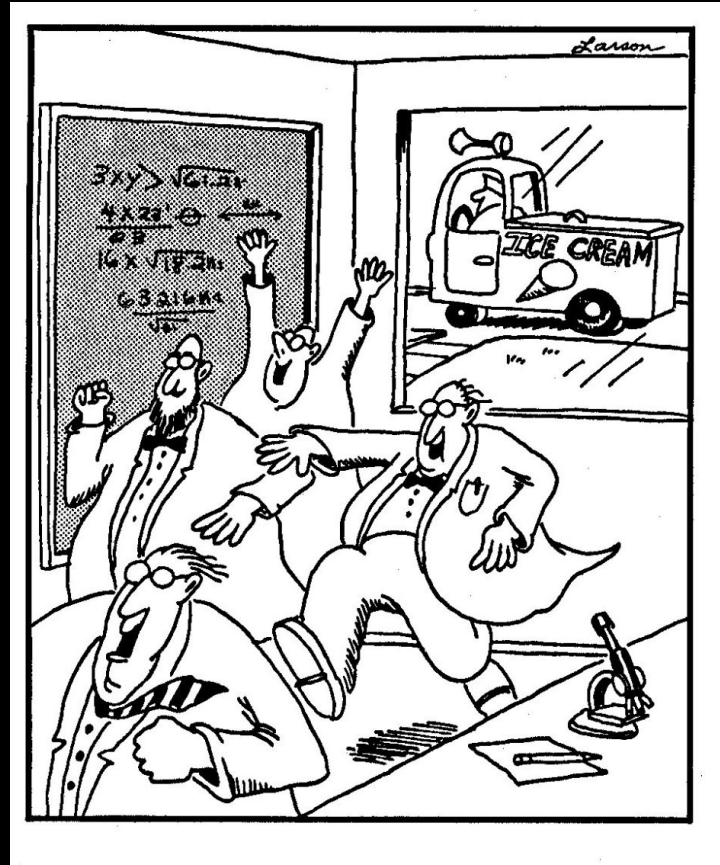
Systematic analysis of IceCube events found an excess of 79 (+22 -20) high-energy neutrinos associated with the nearby **active / starburst galaxy** NGC 1068 at a significance of **4.2  $\sigma$** .

NGC 1068 is a nearby Seyfert II galaxy with a core that is optically thick. It has strong starburst activity and outflows.

Emission scenarios :

- particle acceleration linked to the **active nucleus** (e.g. disk wind) **or starburst region**
- environment allows production of neutrinos and strong absorption of gamma rays

## 5) conclusions & outlook



# variability – attempt at a short summary

---

- Flux variability is detected in all types of AGNs at all wavelengths and time scales (shortest time scales at the highest energies).
- The origin is not clearly understood, but probably **multiple mechanisms** are responsible:
  - geometric effects → long-term variability, QPOs
  - shocks, turbulence in the jet ; variation of the accretion rate → medium- and short-term variability
  - reconnection, turbulence in the jet ; particle acceleration in the BH magnetosphere → very short-term variability
- Links seem to exist between flares and multi-messenger emission, but the correlation is not trivial.  
( high photon density in the source → absorption of gamma-rays, high production of neutrinos  
low photon density in the source → transparency for gamma-rays, low production of neutrinos... )



# what observational approach ?

---

- Need to combine
  - **MWL and VLBI monitoring** of AGNs with regular sampling
    - characterisation of variability at different scales, study of temporal evolution of the jet structure (radio knots...)
  - **MWL and multi-messenger ToOs** on AGN flares
- There is probably a lot more to be learnt from optical and X-ray polarisation studies

# bibliography (section II)

further reading for a deeper understanding ...

